JOURNAL OF MOLECULAR SPECTROSCOPY **169**, 224–242 (1995)

Pure Rotational Spectra of HNCS in the Far Infrared: Ground State Analysis

M. NIEDENHOFF, G. WINNEWISSER, K. M. T. YAMADA, AND S. P. BELOV [1]

I. Physikalisches Institut, Universität zu Köln, D-50937 Cologne, Germany

The pure rotational spectrum of HNCS was recorded under high resolution by a Michelson-type Fourier transform infrared spectrometer in the far-infrared region; also, some high-J submillimeter-wave transitions (e.g., $J = 91 \leftarrow 90$) near 1 THz were observed with the precision of microwave spectroscopy using a high-frequency backward wave oscillator. Effective molecular parameters have been determined for each K_a substate of HNCS up to $K_a = 7$, for DNCS up to $K_a = 6$, for $HNC^{34}S$ up to $K_a = 5$, and for some K_a substates of $HN^{13}CS$ and $H^{15}NCS$, by fitting the available microwave and millimeter-wave transitions simultaneously. The centrifugal distortion resonance has been clearly observed in HNCS and analyzed by a second-order perturbation treatment.

I. INTRODUCTION

Among the molecules exhibiting significantly bent structure, isothiocyanic acid, HNCS, is known as the molecule which manifests most strongly the character of molecular quasilinearity (*1, 2*). The quasilinearity parameter $\gamma_0 = 0.69$ of this molecule is comparable in magnitude to that of fulminic acid, HCNO, which is closer to the linear limit with $\gamma_0 = -0.65$. For the bent limit, the value γ_0 assumes $+1$, and -1 for the linear limit. The molecule HNCS has a fairly large electric dipole moment both in the a and b directions; e.g., for DNCS, both components of the dipole moment have been determined experimentally as $\mu_a = 1.67(3)$ and $\mu_b = 1.08(15)$ D (*3*). Similar values for the dipole moment components are expected to hold for HNCS.

Due to the relative size and direction of the dipole moment, the pure rotational spectrum of this type of molecule is a hybrid spectrum. It consists of a superposition of strong parallel (μ_a dipole transitions) and perpendicular (μ_b dipole transitions) structures. Since the magnitude of the rotational constants, $A \gg B \approx C$, HNCS exhibits very strong a-type spectra ($\Delta K_a = 0$); transitions are therefore found in the microwave (MW), millimeter-wave, and submillimeter-wave (mmW) regions, and strong b-type rotational spectra extend throughout the far-infrared (FIR) region. The perpendicular spectrum is dominated by conspicuous Q branches.

The MW and mmW spectra of this molecule were intensively studied by Yamada and co-workers in 1970s, see, for example, Ref. (*4*); they reported the r_s structure in 1980 (*5*). They have analyzed the transitions of the parallel band together with the perpendicular pure rotational spectra in the FIR region and obtained a fairly complete set of molecular parameters. The FIR spectra were measured by Krakow *et al.* (*6*) using a large grating spectrometer with resolutions between 0.25 and 0.5 cm^{-1}.

The molecular structure was determined from the ground state rotational constants of the various isotopomers, i.e., HNCS, DNCS, $H^{15}NCS$, $HN^{13}CS$, and $HNC^{34}S$; the

[1] On leave of absence from the Microwave Spectroscopy Laboratory, Institute of Applied Physics, Nizhnii Novgorod, Russia.

0022-2852/95 $6.00

HNC angle was found to be 131.7°, and the NCS skeleton, which had been believed to be linear, was discovered to be bent, with an angle of 173.8°.

In the present study, we have remeasured the pure rotational spectra of HNCS both in the FIR by high-resolution Fourier transform and in the terahertz region with microwave techniques. In the FIR region, the present recordings are of much higher resolution (0.00185 cm^{-1}) than that of Krakow *et al.*, and consequently have higher precision (0.05×10^{-3} cm^{-1}) based on the use of the Bruker FTIR spectrometer at Giessen. For the first time, the conspicuous Q branches are partially resolved, revealing details not seen before. Portions of the newly recorded perpendicular spectra near the prominent Q branches are reproduced in Fig. 1.

The newly obtained FIR data contain nearly the complete set of b-type transitions ($\Delta K_a = 1$) up to $K_a = 7 \leftarrow 6$, with which we have been able to determine precise term values for the high-K_a states. However, because of effects of the quasilinearity of the molecule and partly because of the centrifugal distortion resonance (*7*), the line positions of high-K_a rotational levels could not be reproduced by the effective rotational Hamiltonian for asymmetric tops containing a polynomial extension to the higher order terms.

The effect of the centrifugal distortion resonance between the ground state and the $v_5 = 1$ state is clearly observed in the presently recorded FIR spectra and has been analyzed by a second-order perturbation treatment, yielding the interaction constant.

In addition, some a- and b-type transitions have been recorded in the submillimeter-wave region near 1 THz, as shown in Fig. 2, using the new Cologne terahertz spectrometer. The frequency positions of the new submillimeter-wave lines are also included in the analysis, together with the available MW and mmW data.

A portion of the data presented in this paper has been used for determining the quasilinear bending potential by the semirigid-bender model (*8*); the potential hump at the linear position has been found to be about 1000 cm^{-1}, and the energy levels of the excited bending states with $v \geq 2$ have been predicted to be above the potential hump.

II. EXPERIMENTAL PROCEDURES

The high-resolution Fourier transform spectrometer (Bruker IFS-120) at Giessen was employed to record the interferogram for the region from 28 to 350 cm^{-1}. For the present measurements in the FIR region, we used an Si bolometer detector at 4.2 K, a mylar beamsplitter of 12 μm thickness, an Hg lamp as the FIR radiation source, and polyethylene windows. The cell was a 3-m-long Duran glass tube, which was filled with 15 Pa of the sample vapor. The sample of HNCS was prepared by heating a mixture of KSCN and $KHSO_4$, and purified by low-temperature distillation. The 229 interferograms were coadded, and the achieved resolution was 0.00185 cm^{-1}, which is better than that in the previous work of Krakow *et al.* (*6*) by a factor of more than 100. Boxcar apodization and eightfold zero-filling was applied for plotting the spectrum and for measuring the line-center positions.

The line positions were calibrated by selected water lines (*9*) recorded simultaneously as impurity lines, which yielded a precision of 0.05×10^{-3} cm^{-1} for the line-center determination. The accuracy of the line positions thus obtained is limited by that of the water lines used as standards.

A few submillimeter-wave transitions of both a- and b-type have been recorded for the main isotopomer HNCS using a submillimeter backward wave oscillator (BWO) made in Russia (*10*). The output of the BWO (typically 1–10 mW of power) was phase locked to the harmonics of a millimeter-wave synthesizer (KVARZ, Nizhnii

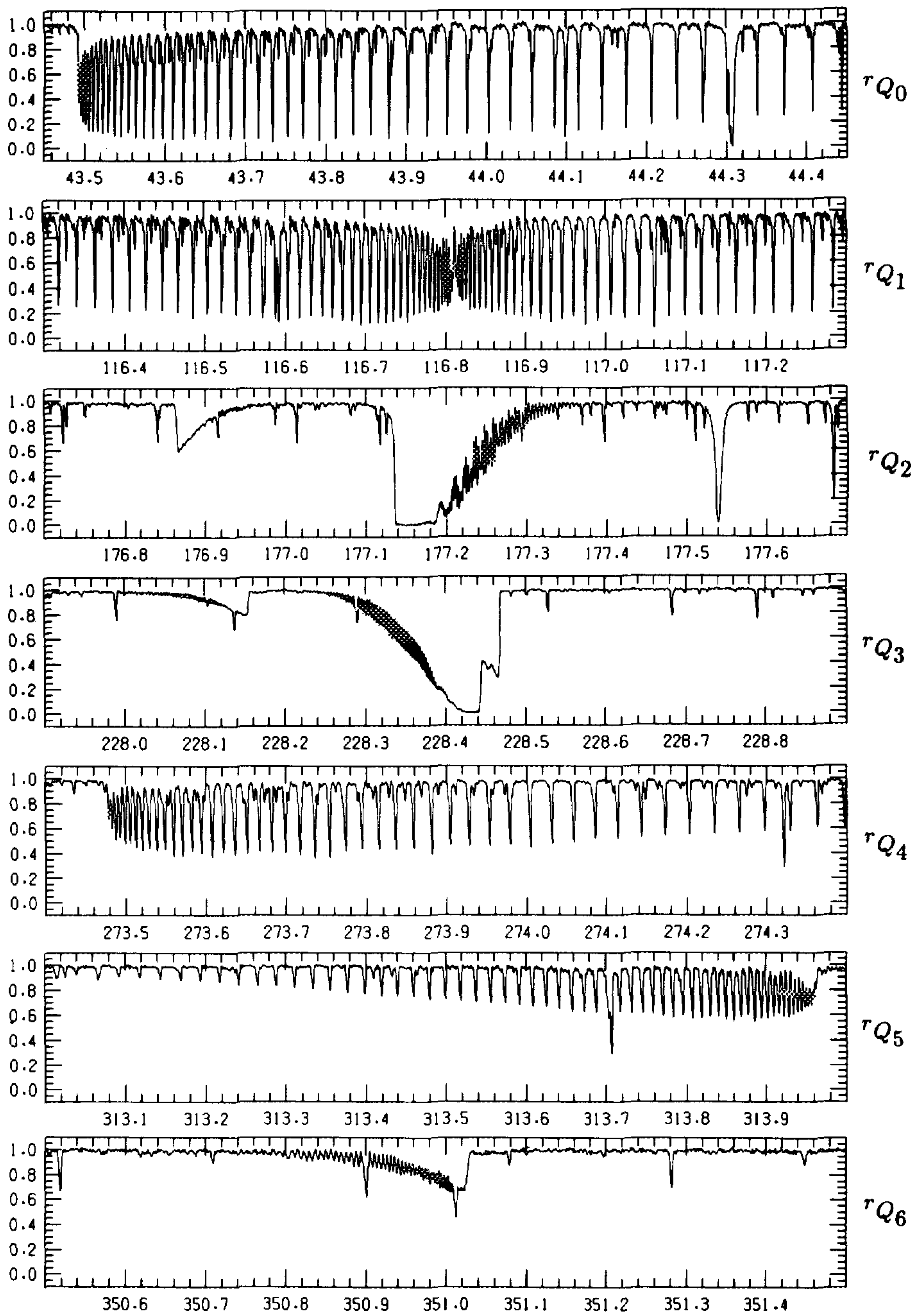

FIG. 1. The observed $^rQ_{K_a}$ transitions of HNCS are reproduced for $K_a'' = 0$ to 6. The magnitude and direction of the degrading changes with increasing K_a quantum number. These anomalous changes in the Q-branch patterns with K_a excitation are mainly due to the centrifugal distortion resonance. The effects of quasilinearity are superimposed (see text).

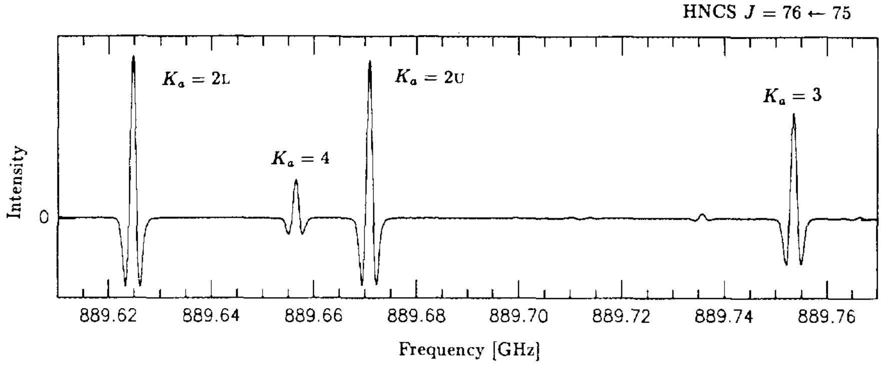

FIG. 2. A portion of the observed submillimeter-wave spectra of HNCS is reproduced; the a-type transition of $J = 76 \leftarrow 75$ with its associated K_a components near 900 GHz are shown. The $K_a = 0$ and the $K_a = 1$ doublets are too far apart in frequency to be shown here.

Novgorod) oscillating around 100 GHz. The spectra have been digitally recorded with a frequency step of 90 or 100 kHz.

III. SPECTRA AND ASSIGNMENTS

Assignments of the ground state lines were easily performed, because the recorded spectra exhibit a typical b-type rotational spectrum of a near-prolate symmetric top with a large rotational constant A. Strong $^rQ_{K_a}$ transitions were clearly observed in the regions reported previously by Krakow *et al.* (6) for $K_a'' = 0$ to 4.

We have extended the assignments up to $K_a'' = 6$. The observed seven Q branches assigned to the ground vibrational state are reproduced in Fig. 1. Associated P- and R-branch transitions were also easily identified.

The principal structure of a perpendicular pure rotational spectrum is well characterized by standard asymmetric rotor theory. For a near-prolate asymmetric-top molecule such as HNCS ($\kappa = -0.99993$), b-type $^rQ_0$ transitions shift the line positions toward higher wavenumbers for increasing J. The $^rQ_1$ branch beautifully exhibits the expected K-type doubling, caused by the inertial asymmetry of the molecule. With increasing J quantum number, the $^rQ_1$-branch lines are split, forming an ascending and a descending branch, depending on the wavenumber. For all other $^rQ_{K_a}$ branches, i.e., those with $K_a \geqslant 2$, the effect of inertial asymmetry recedes and is hardly recognized at the resolution of the FTIR spectrometer.

For the regular case of a near-prolate asymmetric rotor, the expected $^rQ_{K_a}$-branch pattern for $K_a'' \geqslant 2$ is expected to be determined to first order by the effect of centrifugal distortion, i.e., the influence of size and sign of the parameter D_{JK}. Thus the degrading of all higher-K_a Q branches ($K_a'' \geqslant 2$) is expected to be the same. For positive D_{JK} and for increasing J-quantum number, the line positions shift to lower wavenumbers, whereas for negative D_{JK}, the reverse is expected to hold. The standard case with positive D_{JK} is observed for HSSH (*11*). However, for HNCS, the degrading and thus the J pattern of the individual Q branches is far from being that simple, as can be seen in Fig. 1, where we present a composition of all Q branches up to $K_a = 7 \leftarrow 6$. With increasing K_a, the direction and amount of Q-branch degradation shift several times. These anomalies are an unambiguous indication of the centrifugal distortion resonance proposed by Yamada (7) for HNCO, as discussed in Section V below.

In addition to the large number of lines arising from excited bending vibrational states of HNCS, which will be reported in a forthcoming paper, we have identified several isotopomer spectra. Among those are the ground state lines of DNCS commencing with $K_a = 2 \leftarrow 1$ to $K_a = 6 \leftarrow 5$, lines of $HNC^{34}S$ from $K_a = 1 \leftarrow 0$ to $K_a = 5 \leftarrow 4$, and lines of $HN^{13}CS$ and $H^{15}NCS$ for $K_a = 3 \leftarrow 2$. All are observed in natural abundance, except for the D isotopomer which was enriched accidentally by exchange of D on the cell walls. Some of the Q branches assigned to these isotopomers are reproduced in Fig. 3.

IV. ASYMMETRIC ROTOR ANALYSIS

Watson's S-reduced Hamiltonian up to sextic centrifugal distortion terms (12),

$$\begin{aligned}\hat{H}^S_{\mathrm{rot}} = {} & \frac{1}{2}(\tilde{B}^{(S)}_x + \tilde{B}^{(S)}_y)\hat{J}^2 + \left\{\tilde{B}^{(S)}_z - \frac{1}{2}(\tilde{B}^{(S)}_x + \tilde{B}^{(S)}_y)\right\}\hat{J}^2_z \\ & - \Delta_J\hat{J}^4 - \Delta_{JK}\hat{J}^2\hat{J}^2_z - \Delta_K\hat{J}^4_z + H_J\hat{J}^6 + H_{JK}\hat{J}^4\hat{J}^2_z + H_{KJ}\hat{J}^2\hat{J}^4_z + H_K\hat{J}^6_z \\ & + \left\{\frac{1}{4}(\tilde{B}^{(S)}_x - \tilde{B}^{(S)}_y) + d_1\hat{J}^2 + h_1\hat{J}^4\right\}(\hat{J}^2_+ + \hat{J}^2_-) \\ & + (d_2\hat{J}^2 + h_2\hat{J}^4)(\hat{J}^4_+ + \hat{J}^4_-) + h_3(\hat{J}^6_+ + \hat{J}^6_-), \quad (1)\end{aligned}$$

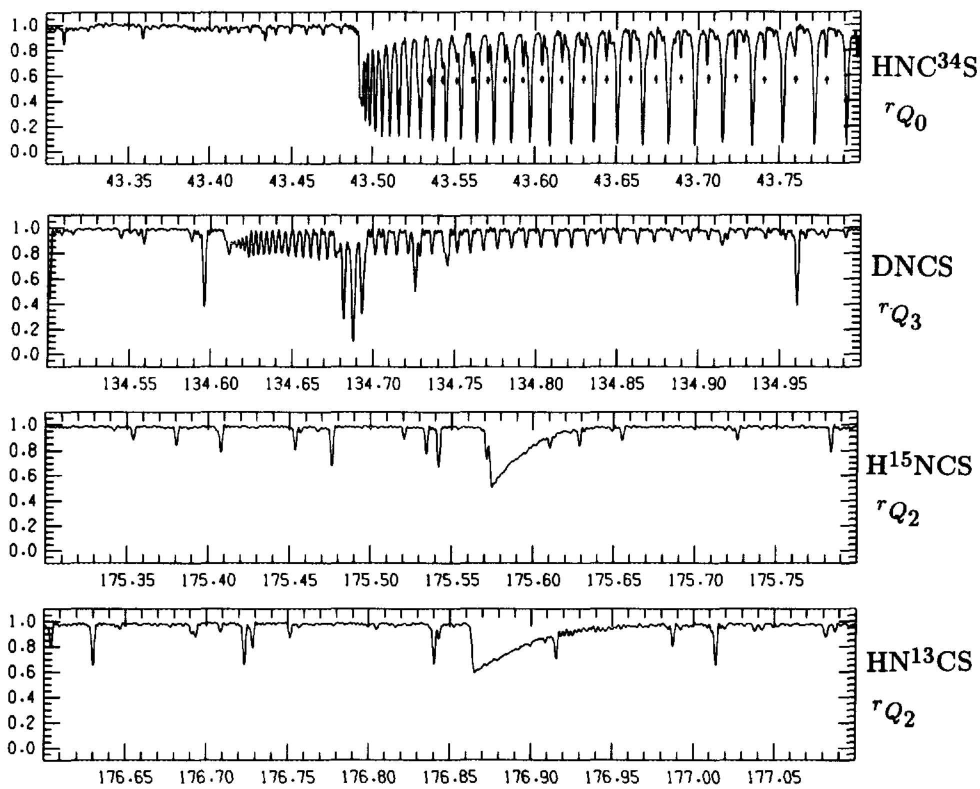

FIG. 3. Observed $^rQ_{K_a}$ transitions of the less abundant isotopomers. From the top down, the $^rQ_0$ lines of $HNC^{34}S$ (marked with arrows) are superimposed on the main species HNCS. The weak Q-branch lines appearing toward lower wavenumbers from the band head near 43.49 cm^{-1} of HNCS are tentatively assigned to $HN^{13}CS$. The $^rQ_3$ lines of DNCS resolved in high J, the unresolved $^rQ_2$ branch of $H^{15}NCS$, and the unresolved $^rQ_2$ branch of $HN^{13}CS$ are degraded to the blue, which also is a manifestation of the centrifugal distortion resonance and the molecular quasilinearity.

TABLE I

Spectroscopic Parameters of HNCS Determined in the Present Study Using a Watson-Type Hamiltonian[a]

	HNCS	$HNC^{34}S$	DNCS	
A	1362.78424(22)	1361.4687(40)	707.58837(27)	GHz
B	5883.462561(38)	5744.83221(38)	5500.43872(19)	MHz
C	5845.611119(38)	5708.73722(41)	5445.22481(19)	MHz
D_J	1.1938893(66)	1.14357(36)	1.09142(29)	kHz
D_{JK}	-1.025240(30)	-1.01693(22)	-1.33344(15)	MHz
D_K	59.33048(27)	57.5857(16)	12.94876(24)	GHz
d_1	-13.78247(73)	-11.27(34)	-34.5575(51)	Hz
d_2	-4.94248(89)	-7.00(27)	-7.89(13)	Hz
H_J	-0.04964(47)	0.0 (fix)	0.0(fix)	Hz
H_{JK}	2.1215(31)	-0.61(12)	3.874(31)	Hz
H_{KJ}	-185.088(16)	-183.232(88)	-120.444(64)	kHz
H_K	6.716261(62)	6.05540(25)	1.067222(51)	GHz
L_{44}	0.7231(15)	-0.1106(70)	0.372(19)	Hz
L_{26}	-16.5450(23)	-16.414(11)	-10.6936(98)	kHz
L_K	464.2044(60)	365.358(17)	67.0713(46)	MHz
S_{46}	0.08109(19)	0.0(fix)	0.0180(17)	Hz
S_{28}	-0.530570(84)	-0.52645(39)	-0.49860(57)	kHz
S_K	17.20156(28)	10.53850(54)	2.39195(20)	MHz
T_{48}	0.0024576(71)	0.0 (fix)	0.000327(41)	Hz
$T_{2,10}$	0.0(fix)	0.0 (fix)	-0.00851(11)	kHz
T_K	0.3144865(60)	0.1128311(60)	0.0428815(43)	MHz
U_K	2.213011(47)	0.0 (fix)	0.298038(33)	kHz

a) The numbers in parentheses represent one standard deviation.

has been extended as described by Yamada and Klee (*13*) to higher order by adding the following terms:

$$\hat{H}' = -L_J\hat{J}^8 - L_{62}\hat{J}^6\hat{J}_z^2 - L_{44}\hat{J}^4\hat{J}_z^4 - L_{26}\hat{J}^2\hat{J}_z^6 - L_K\hat{J}_z^8 + S_J\hat{J}^{10} + S_{82}\hat{J}^8\hat{J}_z^2 + S_{64}\hat{J}^6\hat{J}_z^4 + S_{46}\hat{J}^4\hat{J}_z^6 + S_{28}\hat{J}^2\hat{J}_z^8 + S_K\hat{J}_z^{10} - T_{48}\hat{J}^4\hat{J}_z^8 - T_{2,10}\hat{J}^2\hat{J}_z^{10} - T_K\hat{J}_z^{12} + U_K\hat{J}_z^{14}. \quad (2)$$

TABLE II

Effective Parameters of HNCS for Each K_a State[a]

	$E_0(K)$ in cm^{-1}	B(K) in MHz	D(K) in kHz	H(K) in 10^{-3} Hz
0		5864.536839(38)	1.231063(11)	0.06729(83)
1L	43.49202307(32)	5855.930542(35)	1.1890110(27)	
1U	43.492043(38)	5874.856064(49)	1.2165438(39)	
2L	160.302810(38)	5866.600022(62)	1.194855(12)	-0.02950(84)
2U	160.302807(33)	5866.599768(66)	1.167576(12)	-0.14356(81)
3	337.440421(43)	5867.352796(51)	1.1869585(47)	
4	565.885009(56)	5866.555459(79)	1.171847(33)	-0.1523(32)
5	839.356395(89)	5876.3946(19)	1.21436(31)	
6	1153.32958(12)	5870.3269(30)	1.18880(57)	
7	1504.36319(17)	5868.5608(64)	1.1980(17)	

a) The numbers in parentheses represent one standard deviation. The conversion factor is 1 cm^{-1} = 29979.2458 MHz.

TABLE III

Effective Parameters of DNCS for Each K_a State[a]

	$E_0(K)$ in cm^{-1}	B(K) in MHz	D(K) in kHz	H(K) in 10^{-3} Hz
0		5472.83086(16)	1.23306(25)	0.6906(61)
1L	23.0215651(48)	5460.25079(15)	1.08916(27)	
1U	23.0215626(47)	5487.85804(15)	1.15860(27)	
2L	88.551077(26)	5476.80463(20)	1.10005(34)	
2U	88.551027(26)	5476.80489(19)	0.97396(32)	
3	191.066163(31)	5480.10362(19)	1.05902(32)	
4	325.673266(40)	5483.37740(23)	1.06310(36)	
5	488.481145(50)	5486.28029(29)	1.06986(44)	
6	676.431109(92)	5488.4926(41)	1.0114(15)	

a) The numbers in parentheses represent one standard deviation. The conversion factor is 1 cm^{-1}= 29979.2458 MHz.

Since HNCS is very nearly a prolate symmetric top, $\kappa = -0.99993$, all off-diagonal terms higher than quadratic in the power of J were not required in the present study.

The wavenumber positions of the b-type lines determined in the present study were analyzed together with the new terahertz spectra and the previously reported MW and mmW line positions (*3–5*). Since the $K_a = 5$ levels are strongly perturbed by the centrifugal distortion resonance, as mentioned earlier, the least-squares fit using the above Hamiltonian was carried out for lines limited to $K_a < 5$. For higher-K_a lines, only a single line of the lowest J for each subband was retained in the fit, as was done previously by Yamada *et al.* (*4, 5*). In this way, one obtains the K_a-dependent parameters for predicting the subband origins, without being deceived by the perturbation. The molecular parameters thus obtained are listed in Table I for HNCS, $HNC^{34}S$, and DNCS. Most of the higher order centrifugal distortion correction terms introduced into the above Hamiltonian serve only as fitting parameters with appropriately little physical significance. Nevertheless, the rotational constants A, B, and C determined in this way are reliable for structure calculations. The rotational constant A of $HNC^{34}S$ has been determined for the first time, and that of DNCS has been revised significantly. Otherwise, the constants are in agreement with previously reported values (*5*).

TABLE IV

Effective Parameters of $HNC^{34}S$ for Each K_a State[a]

	$E_0(K)$ in cm^{-1}	B(K) in MHz	D(K) in kHz	H(K) in 10^{-3} Hz	L(K) in 10^{-6} Hz
0		5726.78389(13)	1.17611(24)		
1L	43.491934(47)	5718.60902(11)	1.13827(22)		
1U	43.491954(54)	5736.65796(12)	1.16408(24)		
2L	160.308920(59)	5728.83456(27)	1.13066(89)	7.34(63)	-1.12(12)
2U	160.308655(59)	5728.83403(27)	1.12388(89)	-11.18(62)	1.60(11)
3	337.461131(63)	5729.60674(12)	1.13560(21)		
4	565.930138(76)	5728.87747(17)	1.12259(26)		
5	839.43605(12)	5738.1038(50)	1.1584(17)		

a) The numbers in parentheses represent one standard deviation. The conversion factor is 1 cm^{-1}= 29979.2458 MHz.

TABLE V

Molecular Parameters of $HN^{13}CS$ and $H^{15}NCS$ Determined for $K = 3 \leftarrow 2$ Transitions

	$HN^{13}CS$	$H^{15}NCS$	Unit
$\nu_0(3 \leftarrow 2)$	176.86456(21)	175.574085(74)	cm^{-1}
B(2)	5847.81479(53)	5672.36476(28)	MHz
B(3)	5848.59164(58)	5672.78762(19)	MHz
D(2)	1.1470(23)	1.0935(14)	kHz
D(3)	1.1795(12)	1.10090(36)	kHz
H(2)	−1.59(28)	−7.6(22)	10^{-3} Hz

a) The numbers in parentheses represent one standard deviation. The conversion factor is 1 cm^{-1}= 29979.2458 MHz.

The Watson-type effective Hamiltonian is not appropriate for high-K_a transitions of HNCS, because of the effect of quasilinearity and the influence of the centrifugal distortion resonance. Thus, in the present study, we have determined the spectroscopic parameters for each K_a substate, given individually in those cases where the K-type doublings are resolved (for $K_a = 1$ and 2). Thus, the well known energy expression for linear molecules has been employed using K in place of K_a,

$$E(J, K, \gamma) = E_0(K) + B(K, \gamma)J(J+1) - D(K, \gamma)J^2(J+1)^2 + H(K, \gamma)J^3(J+1)^3 - L(K, \gamma)J^4(J+1)^4, \quad (3)$$

where the energy contribution of the K rotation is represented by E_0, and B is the effective rotational constant. The D, H, and L terms are the centrifugal distortion corrections for the given K substate, and γ is the index for the K doublet (U for upper, L for the lower component). The K-doublet index γ is omitted if no doubling is observed.

The parameters determined by the least-squares fits are collected in Tables II–V for HNCS, DNCS, $HNC^{34}S$, $HN^{13}CS$, and $H^{15}NCS$, respectively. The experimental line positions of the main isotopomer are listed in Table VI together with the observed − calculated values. For the other isotopomers, such a list is available from the authors upon request.[2] The newly measured a- and b-type submillimeter-wave lines near 1 THz are summarized in Table VII.

V. CENTRIFUGAL DISTORTION RESONANCE

Figure 4 illustrates the K_a dependence of the effective rotational constant B thus determined. In this figure, the average of the B values for the K doublets is used in the cases $K_a = 1$ and 2. This figure suggests a typical avoided crossing of energy levels in a resonance system between $K_a = 4$ and 5. The ground state K_a-rotational energy terms are plotted in Fig. 5 together with those of the lowest three excited bending vibrations. Locations of the levels of the three excited states have been determined from the presently recorded spectra by assigning lines of the excited states and several forbidden transitions between the vibrational states, which will be presented in a forthcoming paper.

The centrifugal distortion resonance proposed by Yamada (7) couples the rotational levels of the ground state (gs) with those of the lowest excited vibrational state (v_5 =

[2] Also on deposit in the Editorial Office of this journal.

TABLE VI

Observed Line Positions of HNCS in cm^{-1} Measured by FTIR Spectroscopy[a]

Transition	Freq.	Δ	Transition	Freq.	Δ	Transition	Freq.	Δ	Transition	Freq.	Δ
Qrp (2, 0, 2)	43.49374	-37	Qrp (72, 0, 72)	45.31427	-1	Rrr (11, 0, 11)	48.14189	2	Rrr (83, 0, 83)	74.27971	-12
Qrp (3, 0, 3)	43.49616	-1				Rrr (12, 0, 12)	48.52562	4			
Qrp (4, 0, 4)	43.49889	-4	Prp (57, 0, 57)	20.31946	-18	Rrr (13, 0, 13)	48.90874	3	Qrp (70, 1, 69)	115.48174	-4
Qrp (5, 0, 5)	43.50225	-12	Prp (56, 0, 56)	20.74033	-15	Rrr (14, 0, 14)	49.29130	5	Qrp (69, 1, 68)	115.51812	-2
Qrp (6, 0, 6)	43.50650	0	Prp (55, 0, 55)	21.16114	28	Rrr (15, 0, 15)	49.67325	4	Qrp (68, 1, 67)	115.55406	1
Qrp (7, 0, 7)	43.51123	-9	Prp (54, 0, 54)	21.58088	12	Rrr (16, 0, 16)	50.05462	4	Qrp (67, 1, 66)	115.58947	-2
Qrp (8, 0, 8)	43.51683	0	Prp (53, 0, 53)	22.00022	3	Rrr (17, 0, 17)	50.43542	5	Qrp (66, 1, 65)	115.62444	-3
Qrp (9, 0, 9)	43.52306	3	Prp (52, 0, 52)	22.41907	-8	Rrr (18, 0, 18)	50.81560	3	Qrp (65, 1, 64)	115.65895	-3
Qrp (10, 0, 10)	43.52990	-1	Prp (51, 0, 51)	22.83773	11	Rrr (19, 0, 19)	51.19523	5	Qrp (64, 1, 63)	115.69286	-16
Qrp (11, 0, 11)	43.53753	4	Prp (50, 0, 50)	23.25572	11	Rrr (20, 0, 20)	51.57425	4	Qrp (63, 1, 62)	115.72652	-7
Qrp (12, 0, 12)	43.54581	6	Prp (49, 0, 49)	23.67317	5	Rrr (21, 0, 21)	51.95270	5	Qrp (62, 1, 61)	115.75963	-5
Qrp (13; 0, 13)	43.55470	-1	Prp (48, 0, 48)	24.09028	12	Rrr (22, 0, 22)	52.33056	6	Qrp (61, 1, 60)	115.79223	-7
Qrp (14, 0, 14)	43.56437	2	Prp (47, 0, 47)	24.50674	6	Rrr (23, 0, 23)	52.70780	3	Qrp (60, 1, 59)	115.82443	-1
Qrp (15, 0, 15)	43.57475	7	Prp (46, 0, 46)	24.92274	2	Rrr (24, 0, 24)	53.08448	4	Qrp (59, 1, 58)	115.85606	-4
Qrp (16, 0, 16)	43.58567	-3	Prp (45, 0, 45)	25.33838	11	Rrr (25, 0, 25)	53.46057	4	Qrp (58, 1, 57)	115.88724	-4
Qrp (17, 0, 17)	43.59746	4	Prp (44, 0, 44)	25.75361	29	Rrr (26, 0, 26)	53.83608	4	Qrp (57, 1, 56)	115.91793	-4
Qrp (18, 0, 18)	43.60989	7	Prp (43, 0, 43)	26.16813	25	Rrr (27, 0, 27)	54.21101	6	Qrp (56, 1, 55)	115.94813	-4
Qrp (19, 0, 19)	43.62291	0	Prp (42, 0, 42)	26.58206	14	Rrr (28, 0, 28)	54.58531	3	Qrp (55, 1, 54)	115.97787	-2
Qrp (20, 0, 20)	43.63671	1	Prp (41, 0, 41)	26.99565	18	Rrr (29, 0, 29)	54.95907	6	Qrp (54, 1, 53)	116.00707	-4
Qrp (21, 0, 21)	43.65120	3	Prp (40, 0, 40)	27.40862	11	Rrr (30, 0, 30)	55.33223	7	Qrp (53, 1, 52)	116.03582	-1
Qrp (22, 0, 22)	43.66636	2	Prp (39, 0, 39)	27.82114	10	Rrr (32, 0, 32)	56.07672	2	Qrp (52, 1, 51)	116.06406	-1
Qrp (23, 0, 23)	43.68219	-1	Prp (38, 0, 38)	28.23317	11	Rrr (33, 0, 33)	56.44811	3	Qrp (51, 1, 50)	116.09180	0
Qrp (24, 0, 24)	43.69877	3	Prp (37, 0, 37)	28.64456	-1	Rrr (34, 0, 34)	56.81891	3	Qrp (50, 1, 49)	116.11901	-2
Qrp (25, 0, 25)	43.71598	-1	Prp (36, 0, 36)	29.05554	-2	Rrr (35, 0, 35)	57.18918	9	Qrp (49, 1, 48)	116.14582	5
Qrp (26, 0, 26)	43.73396	4	Prp (35, 0, 35)	29.46596	-8	Rrr (36, 0, 36)	57.55879	7	Qrp (48, 1, 47)	116.17197	-3
Qrp (27, 0, 27)	43.75257	3	Prp (34, 0, 34)	29.87605	6	Rrr (37, 0, 37)	57.92779	4	Qrp (47, 1, 46)	116.19771	-1
Qrp (28, 0, 28)	43.77188	2	Prp (33, 0, 33)	30.28546	4	Rrr (38, 0, 38)	58.29627	7	Qrp (46, 1, 45)	116.22294	1
Qrp (29, 0, 29)	43.79190	3	Prp (32, 0, 32)	30.69435	2	Rrr (39, 0, 39)	58.66413	7	Qrp (45, 1, 44)	116.24767	3
Qrp (30, 0, 30)	43.81260	2	Prp (31, 0, 31)	31.10263	-8	Rrr (40, 0, 40)	59.03138	4	Qrp (44, 1, 43)	116.27182	-2
Qrp (31, 0, 31)	43.83401	3	Prp (30, 0, 30)	31.51065	8	Rrr (41, 0, 41)	59.39809	6	Qrp (43, 1, 42)	116.29550	-2
Qrp (32, 0, 32)	43.85609	2	Prp (29, 0, 29)	31.91798	9	Rrr (42, 0, 42)	59.76423	9	Qrp (42, 1, 41)	116.31871	2
Qrp (33, 0, 33)	43.87889	3	Prp (28, 0, 28)	32.32474	5	Rrr (43, 0, 43)	60.12971	5	Qrp (41, 1, 40)	116.34133	-1
Qrp (34, 0, 34)	43.90237	3	Prp (27, 0, 27)	32.73097	2	Rrr (44, 0, 44)	60.49466	7	Qrp (40, 1, 39)	116.36345	-3
Qrp (35, 0, 35)	43.92673	21	Prp (26, 0, 26)	33.13673	6	Rrr (45, 0, 45)	60.85903	8	Qrp (39, 1, 38)	116.38506	-4
Qrp (36, 0, 36)	43.95141	2	Prp (25, 0, 25)	33.54198	12	Rrr (46, 0, 46)	61.22276	5	Qrp (38, 1, 37)	116.40620	1
Qrp (37, 0, 37)	43.97695	-1	Prp (24, 0, 24)	33.94654	4	Rrr (47, 0, 47)	61.58597	7	Qrp (37, 1, 36)	116.42677	0
Qrp (38, 0, 38)	44.00327	5	Prp (23, 0, 23)	34.35067	6	Rrr (48, 0, 48)	61.94857	7	Qrp (36, 1, 35)	116.44684	2
Qrp (39, 0, 39)	44.03024	6	Prp (22, 0, 22)	34.75413	-4	Rrr (49, 0, 49)	62.31054	1	Qrp (35, 1, 34)	116.46639	5
Qrp (40, 0, 40)	44.05788	4	Prp (21, 0, 21)	35.15726	8	Rrr (50, 0, 50)	62.67222	25	Qrp (34, 1, 33)	116.48537	3
Qrp (41, 0, 41)	44.08623	3	Prp (20, 0, 20)	35.55971	5	Rrr (51, 0, 51)	63.03293	10	Qrp (33, 1, 32)	116.50381	0
Qrp (42, 0, 42)	44.11535	9	Prp (19, 0, 19)	35.96156	-2	Rrr (52, 0, 52)	63.39321	10	Qrp (32, 1, 31)	116.52176	0
Qrp (43, 0, 43)	44.14512	11	Prp (18, 0, 18)	36.36296	1	Rrr (53, 0, 53)	63.75290	9	Qrp (31, 1, 30)	116.53927	10
Qrp (44, 0, 44)	44.17549	2	Prp (17, 0, 17)	36.76379	2	Rrr (54, 0, 54)	64.11202	8	Qrp (30, 1, 29)	116.55617	12
Qrp (45, 0, 45)	44.20661	-1	Prp (16, 0, 16)	37.16405	1	Rrr (55, 0, 55)	64.47061	12	Qrp (29, 1, 28)	116.57247	7
Qrp (46, 0, 46)	44.23850	3	Prp (15, 0, 15)	37.56384	8	Rrr (56, 0, 56)	64.82858	12	Qrp (28, 1, 27)	116.58826	5
Qrp (47, 0, 47)	44.27106	3	Prp (14, 0, 14)	37.96299	7	Rrr (57, 0, 57)	65.18597	11	Qrp (27, 1, 26)	116.60350	1
Qrp (48, 0, 48)	44.30441	12	Prp (13, 0, 13)	38.36157	5	Rrr (58, 0, 58)	65.54278	10	Qrp (26, 1, 25)	116.61821	-3
Qrp (49, 0, 49)	44.33829	5	Prp (12, 0, 12)	38.75962	6	Rrr (59, 0, 59)	65.89907	14	Qrp (25, 1, 24)	116.63242	-2
Qrp (50, 0, 50)	44.37301	11	Prp (11, 0, 11)	39.15706	2	Rrr (60, 0, 60)	66.25473	12	Qrp (24, 1, 23)	116.64613	2
Qrp (51, 0, 51)	44.40831	5	Prp (10, 0, 10)	39.55398	2	Rrr (61, 0, 61)	66.60982	11	Qrp (23, 1, 22)	116.65932	8
Qrp (52, 0, 52)	44.44437	5	Prp (9, 0, 9)	39.95040	8	Rrr (62, 0, 62)	66.96432	8	Qrp (22, 1, 21)	116.67192	9
Qrp (53, 0, 53)	44.48115	6	Prp (8, 0, 8)	40.34613	1	Rrr (63, 0, 63)	67.31834	12	Qrp (21, 1, 20)	116.68401	12
Qrp (54, 0, 54)	44.51860	3	Prp (7, 0, 7)	40.74139	4	Rrr (64, 0, 64)	67.67168	8	Qrp (20, 1, 19)	116.69543	5
Qrp (55, 0, 55)	44.55670	-5	Prp (6, 0, 6)	41.13606	5	Rrr (65, 0, 65)	68.02463	20	Qrp (19, 1, 18)	116.70655	20
Qrp (56, 0, 56)	44.59566	3	Prp (5, 0, 5)	41.53023	12	Rrr (66, 0, 66)	68.37682	12	Qrp (18, 1, 17)	116.71697	20
Qrp (57, 0, 57)	44.63528	6	Prp (4, 0, 4)	41.92365	2	Rrr (67, 0, 67)	68.72847	8	Qrp (17, 1, 16)	116.72687	23
Qrp (58, 0, 58)	44.67554	2	Prp (3, 0, 3)	42.31663	4	Rrr (68, 0, 68)	69.07969	16	Qrp (16, 1, 15)	116.73616	18
Qrp (59, 0, 59)	44.71656	3	Prp (2, 0, 2)	42.70893	-4	Rrr (69, 0, 69)	69.43032	22	Qrp (15, 1, 14)	116.74493	17
Qrp (60, 0, 60)	44.75831	7				Rrr (70, 0, 70)	69.78024	12	Qrp (14, 1, 13)	116.75319	19
Qrp (61, 0, 61)	44.80065	-1	Rrr (0, 0, 0)	43.88303	34	Rrr (71, 0, 71)	70.12970	14	Qrp (13, 1, 12)	116.76079	9
Qrp (62, 0, 62)	44.84384	5	Rrr (1, 0, 1)	44.27297	19	Rrr (72, 0, 72)	70.47853	7	Qrp (12, 1, 11)	116.76796	12
Qrp (63, 0, 63)	44.88768	5	Rrr (2, 0, 2)	44.66238	9	Rrr (73, 0, 73)	70.82693	14	Qrp (11, 1, 10)	116.77457	12
Qrp (64, 0, 64)	44.93222	3	Rrr (3, 0, 3)	45.05126	3	Rrr (74, 0, 74)	71.17466	9	Qrp (10, 1, 9)	116.78057	8
Qrp (65, 0, 65)	44.97756	11	Rrr (4, 0, 4)	45.43960	1	Rrr (75, 0, 75)	71.52192	12	Qrp (9, 1, 8)	116.78594	-5
Qrp (66, 0, 66)	45.02348	5	Rrr (5, 0, 5)	45.82741	4	Rrr (76, 0, 76)	71.86887	40	Qrp (8, 1, 7)	116.79092	-2
Qrp (67, 0, 67)	45.07019	7	Rrr (6, 0, 6)	46.21458	1	Rrr (77, 0, 77)	72.21472	12	Qrp (7, 1, 6)	116.79544	9
Qrp (68, 0, 68)	45.11759	7	Rrr (7, 0, 7)	46.60127	7	Rrr (78, 0, 78)	72.56029	12	Qrp (6, 1, 5)	116.79910	-10
Qrp (69, 0, 69)	45.16574	10	Rrr (8, 0, 8)	46.98726	2	Rrr (79, 0, 79)	72.90534	15	Qrp (5, 1, 4)	116.80253	3
Qrp (70, 0, 70)	45.21444	-3	Rrr (9, 0, 9)	47.37273	3	Rrr (80, 0, 80)	73.25028	61	Qrp (4, 1, 3)	116.80538	12
Qrp (71, 0, 71)	45.26415	14	Rrr (10, 0, 10)	47.75763	6	Rrr (82, 0, 82)	73.93729	29	Qrp (3, 1, 2)	116.80791	45

[a])Transitions are indicated by ΔJ, ΔK_a, and ΔK_c, followed by the lower state quantum numbers J'', K_a'', and K_c'' in parentheses. Capital P, Q, and R represent $\Delta J = -1$, 0, and +1, respectively. Lower case p, q, and r are used to indicate ΔK_a and ΔK_c. Observed line positions are listed in the column of "Freq.". The observed–calculated values are in the column of Δ in the unit of 10^{-5} cm^{-1}.

1) with the selection rule $\Delta K_a = \pm 1$. As indicated in Fig. 5, the $K_a = 4$ (gs) level is located slightly lower than the coupling partner of $K_a = 3$ ($v_5 = 1$). The $K_a = 5$ (gs) level is very close to the $K_a = 4$ ($v_5 = 1$) level, but in this case the former level is

TABLE VI—*Continued*

Transition	Freq.	Δ	Transition	Freq.	Δ	Transition	Freq.	Δ	Transition	Freq.	Δ
Qrp (2, 1, 2)	116.81275	-17	Qrp (74, 1, 74)	118.77978	-5	Prp (18, 1, 17)	109.67283	3	Rrr (54, 1, 53)	137.49849	5
Qrp (3, 1, 3)	116.81503	-3	Qrp (75, 1, 75)	118.83277	-11	Prp (17, 1, 16)	110.07395	2	Rrr (55, 1, 54)	137.85849	-4
Qrp (4, 1, 4)	116.81805	15	Qrp (76, 1, 76)	118.88646	-16	Prp (16, 1, 15)	110.47452	-1	Rrr (56, 1, 55)	138.21801	-3
Qrp (5, 1, 5)	116.82128	-18	Qrp (77, 1, 77)	118.94093	-12	Prp (15, 1, 14)	110.87461	2	Rrr (57, 1, 56)	138.57695	-2
Qrp (6, 1, 6)	116.82583	10	Qrp (78, 1, 78)	118.99604	-14	Prp (14, 1, 13)	111.27413	1	Rrr (58, 1, 57)	138.93533	0
Qrp (7, 1, 7)	116.83084	12				Prp (13, 1, 12)	111.67313	2	Rrr (59, 1, 58)	139.29308	-3
Qrp (8, 1, 8)	116.83632	-9	Prp (85, 1, 84)	81.66670	-8	Prp (12, 1, 11)	112.07160	3	Rrr (60, 1, 59)	139.65028	-3
Qrp (9, 1, 9)	116.84270	-12	Prp (83, 1, 82)	82.53283	41	Prp (11, 1, 10)	112.46951	2	Rrr (61, 1, 60)	140.00693	0
Qrp (10, 1, 10)	116.85000	7	Prp (81, 1, 80)	83.39619	-23	Prp (10, 1, 9)	112.86690	3	Rrr (62, 1, 61)	140.36294	-3
Qrp (11, 1, 11)	116.85770	-6	Prp (80, 1, 79)	83.82766	-12	Prp (9, 1, 8)	113.26375	4	Rrr (63, 1, 62)	140.71816	-28
Qrp (12, 1, 12)	116.86635	5	Prp (78, 1, 77)	84.68896	-31	Prp (8, 1, 7)	113.66005	5	Rrr (64, 1, 63)	141.07328	-5
Qrp (13, 1, 13)	116.87560	5	Prp (77, 1, 76)	85.11938	0	Prp (7, 1, 6)	114.05580	4	Rrr (65, 1, 64)	141.42762	-2
Qrp (14, 1, 14)	116.88555	3	Prp (76, 1, 75)	85.54894	-12	Prp (6, 1, 5)	114.45101	4	Rrr (66, 1, 65)	141.78132	-6
Qrp (15, 1, 15)	116.89618	-1	Prp (75, 1, 74)	85.97858	25	Prp (5, 1, 4)	114.84570	6	Rrr (67, 1, 66)	142.13446	-7
Qrp (16, 1, 16)	116.90761	3	Prp (74, 1, 73)	86.40690	-24	Prp (4, 1, 3)	115.23975	-1	Rrr (68, 1, 67)	142.48710	-1
Qrp (17, 1, 17)	116.91979	12	Prp (73, 1, 72)	86.83545	-9	Prp (3, 1, 2)	115.63328	-5	Rrr (69, 1, 68)	142.83910	-2
Qrp (18, 1, 18)	116.93263	15	Prp (72, 1, 71)	87.26347	-2				Rrr (70, 1, 69)	143.19048	-7
Qrp (19, 1, 19)	116.94607	7	Prp (71, 1, 70)	87.69088	-12	Rrr (1, 1, 0)	117.59361	64	Rrr (71, 1, 70)	143.54131	-9
Qrp (20, 1, 20)	116.96023	0	Prp (70, 1, 69)	88.11801	-8	Rrr (2, 1, 1)	117.98349	25	Rrr (72, 1, 71)	143.89156	-11
Qrp (21, 1, 21)	116.97499	-18	Prp (69, 1, 68)	88.54469	-4	Rrr (3, 1, 2)	118.37302	6	Rrr (73, 1, 72)	144.24137	0
Qrp (22, 1, 22)	116.99065	-17	Prp (68, 1, 67)	88.97089	-3	Rrr (4, 1, 3)	118.76219	6	Rrr (74, 1, 73)	144.59046	-3
Qrp (23, 1, 23)	117.00718	0	Prp (67, 1, 66)	89.39663	-4	Rrr (5, 1, 4)	119.15080	6	Rrr (75, 1, 74)	144.93896	-8
Qrp (24, 1, 24)	117.02425	0	Prp (66, 1, 65)	89.82186	-12	Rrr (6, 1, 5)	119.53866	-12	Rrr (76, 1, 75)	145.28699	-3
Qrp (25, 1, 25)	117.04200	-4	Prp (65, 1, 64)	90.24668	-15	Rrr (7, 1, 6)	119.92632	4	Rrr (77, 1, 76)	145.63440	-1
Qrp (26, 1, 26)	117.06114	61	Prp (64, 1, 63)	90.67115	-8	Rrr (8, 1, 7)	120.31327	5	Rrr (78, 1, 77)	145.98121	-3
Qrp (27, 1, 27)	117.07974	1	Prp (63, 1, 62)	91.09516	-1	Rrr (9, 1, 8)	120.69962	2	Rrr (79, 1, 78)	146.32832	83
Qrp (28, 1, 28)	117.09962	-2	Prp (62, 1, 61)	91.51865	-2	Rrr (10, 1, 9)	121.08544	2	Rrr (80, 1, 79)	146.67313	-3
Qrp (29, 1, 29)	117.12029	2	Prp (61, 1, 60)	91.94161	-9	Rrr (11, 1, 10)	121.47072	4	Rrr (81, 1, 80)	147.01839	12
Qrp (30, 1, 30)	117.14160	0	Prp (60, 1, 59)	92.36422	-5	Rrr (12, 1, 11)	121.85548	10	Rrr (82, 1, 81)	147.36287	7
Qrp (31, 1, 31)	117.16363	-1	Prp (59, 1, 58)	92.78632	-6	Rrr (13, 1, 12)	122.23953	1	Rrr (83, 1, 82)	147.70670	-6
Qrp (32, 1, 32)	117.18641	2	Prp (58, 1, 57)	93.20797	-6	Rrr (14, 1, 13)	122.62316	7	Rrr (84, 1, 83)	148.05009	-5
Qrp (33, 1, 33)	117.20985	0	Prp (57, 1, 56)	93.62920	-1	Rrr (15, 1, 14)	123.00613	3	Rrr (85, 1, 84)	148.39291	-4
Qrp (34, 1, 34)	117.23402	0	Prp (56, 1, 55)	94.04988	-4	Rrr (16, 1, 15)	123.38851	-4	Rrr (86, 1, 85)	148.73519	-1
Qrp (35, 1, 35)	117.25890	0	Prp (55, 1, 54)	94.47011	-5	Rrr (17, 1, 16)	123.77046	3	Rrr (87, 1, 86)	149.07675	-12
Qrp (36, 1, 36)	117.28449	0	Prp (54, 1, 53)	94.88985	-8	Rrr (18, 1, 17)	124.15181	7	Rrr (91, 1, 90)	150.43748	-38
Qrp (37, 1, 37)	117.31076	-3	Prp (53, 1, 52)	95.30908	-15	Rrr (19, 1, 18)	124.53257	8			
Qrp (38, 1, 38)	117.33779	0	Prp (52, 1, 51)	95.72796	-9	Rrr (20, 1, 19)	124.91271	3	Prn (81, 1, 81)	87.58591	-12
Qrp (39, 1, 39)	117.36549	-2	Prp (51, 1, 50)	96.14641	1	Rrr (21, 1, 20)	125.29233	3	Prn (80, 1, 80)	87.91534	3
Qrp (40, 1, 40)	117.39391	-2	Prp (50, 1, 49)	96.56425	-1	Rrr (22, 1, 21)	125.67138	4	Prn (79, 1, 79)	88.24525	-17
Qrp (41, 1, 41)	117.42303	-3	Prp (49, 1, 48)	96.98163	-2	Rrr (23, 1, 22)	126.04983	1	Prn (77, 1, 77)	88.90791	-22
Qrp (42, 1, 42)	117.45288	-1	Prp (48, 1, 47)	97.39850	-5	Rrr (24, 1, 23)	126.42777	3	Prn (76, 1, 76)	89.24078	5
Qrp (43, 1, 43)	117.48341	-3	Prp (47, 1, 46)	97.81493	-4	Rrr (25, 1, 24)	126.80569	61	Prn (75, 1, 75)	89.57423	6
Qrp (44, 1, 44)	117.51467	-2	Prp (46, 1, 45)	98.23089	-1	Rrr (26, 1, 25)	127.18194	9	Prn (74, 1, 74)	89.90826	-16
Qrp (45, 1, 45)	117.54660	-5	Prp (45, 1, 44)	98.64631	-3	Rrr (27, 1, 26)	127.55808	3	Prn (73, 1, 73)	90.24349	-2
Qrp (46, 1, 46)	117.57929	-2	Prp (44, 1, 43)	99.06130	1	Rrr (28, 1, 27)	127.93373	5	Prn (72, 1, 72)	90.57948	7
Qrp (47, 1, 47)	117.61267	-1	Prp (43, 1, 42)	99.47576	1	Rrr (29, 1, 28)	128.30877	3	Prn (71, 1, 71)	90.91604	-9
Qrp (48, 1, 48)	117.64673	-3	Prp (42, 1, 41)	99.88971	-1	Rrr (30, 1, 29)	128.68324	1	Prn (70, 1, 70)	91.25349	-19
Qrp (49, 1, 49)	117.68153	-2	Prp (41, 1, 40)	100.30322	2	Rrr (31, 1, 30)	129.05717	3	Prn (69, 1, 69)	91.59198	-6
Qrp (50, 1, 50)	117.71701	-3	Prp (40, 1, 39)	100.71614	-3	Rrr (32, 1, 31)	129.43052	4	Prn (68, 1, 68)	91.93117	-4
Qrp (51, 1, 51)	117.75319	-4	Prp (39, 1, 38)	101.12864	-1	Rrr (33, 1, 32)	129.80320	-5	Prn (67, 1, 67)	92.27112	-8
Qrp (52, 1, 52)	117.79014	1	Prp (38, 1, 37)	101.54058	-5	Rrr (34, 1, 33)	130.17547	2	Prn (66, 1, 66)	92.61191	-9
Qrp (53, 1, 53)	117.82777	3	Prp (37, 1, 36)	101.95209	-1	Rrr (35, 1, 34)	130.54711	4	Prn (65, 1, 65)	92.95353	-7
Qrp (54, 1, 54)	117.86597	-8	Prp (36, 1, 35)	102.36308	0	Rrr (36, 1, 35)	130.91814	3	Prn (64, 1, 64)	93.29593	-9
Qrp (55, 1, 55)	117.90499	-8	Prp (35, 1, 34)	102.77354	0	Rrr (37, 1, 36)	131.28859	0	Prn (63, 1, 63)	93.63917	-6
Qrp (56, 1, 56)	117.94478	-1	Prp (34, 1, 33)	103.18349	-2	Rrr (38, 1, 37)	131.65850	2	Prn (62, 1, 62)	93.98317	-9
Qrp (58, 1, 58)	118.02626	-8	Prp (33, 1, 32)	103.59296	0	Rrr (39, 1, 38)	132.02781	0	Prn (61, 1, 61)	94.32793	-15
Qrp (59, 1, 59)	118.06810	-7	Prp (32, 1, 31)	104.00191	1	Rrr (40, 1, 39)	132.39655	0	Prn (60, 1, 60)	94.67367	-3
Qrp (60, 1, 60)	118.11067	-4	Prp (31, 1, 30)	104.41038	4	Rrr (41, 1, 40)	132.76470	-2	Prn (59, 1, 59)	95.02003	-9
Qrp (61, 1, 61)	118.15391	-3	Prp (30, 1, 29)	104.81819	-7	Rrr (42, 1, 41)	133.13230	-2	Prn (58, 1, 58)	95.36730	-3
Qrp (62, 1, 62)	118.19781	-7	Prp (29, 1, 28)	105.22569	2	Rrr (43, 1, 42)	133.49934	1	Prn (57, 1, 57)	95.71532	-2
Qrp (63, 1, 63)	118.24242	-10	Prp (28, 1, 27)	105.63260	4	Rrr (44, 1, 43)	133.86579	2	Prn (55, 1, 55)	96.41365	-8
Qrp (64, 1, 64)	118.28778	-9	Prp (27, 1, 26)	106.03896	3	Rrr (45, 1, 44)	134.23162	-2	Prn (54, 1, 54)	96.76404	-7
Qrp (65, 1, 65)	118.33383	-8	Prp (26, 1, 25)	106.44479	0	Rrr (46, 1, 45)	134.59693	0	Prn (53, 1, 53)	97.11524	-4
Qrp (66, 1, 66)	118.38058	-8	Prp (25, 1, 24)	106.84998	-14	Rrr (47, 1, 46)	134.96160	-4	Prn (52, 1, 52)	97.46722	-1
Qrp (67, 1, 67)	118.42795	-16	Prp (24, 1, 23)	107.25498	4	Rrr (48, 1, 47)	135.32577	0	Prn (51, 1, 51)	97.81996	0
Qrp (68, 1, 68)	118.47615	-11	Prp (23, 1, 22)	107.65916	-7	Rrr (49, 1, 48)	135.68931	-2	Prn (50, 1, 50)	98.17345	-3
Qrp (69, 1, 69)	118.52503	-7	Prp (22, 1, 21)	108.06301	1	Rrr (50, 1, 49)	136.05229	-1	Prn (49, 1, 49)	98.52775	-2
Qrp (70, 1, 70)	118.57456	-9	Prp (21, 1, 20)	108.46629	5	Rrr (51, 1, 50)	136.41468	-2	Prn (48, 1, 48)	98.88283	-1
Qrp (71, 1, 71)	118.62479	-11	Prp (20, 1, 19)	108.86900	4	Rrr (52, 1, 51)	136.77652	-1	Prn (47, 1, 47)	99.23867	-2
Qrp (73, 1, 73)	118.72764	15	Prp (19, 1, 18)	109.27117	3	Rrr (53, 1, 52)	137.13777	0	Prn (46, 1, 46)	99.59528	-3

higher in energy. Thus, if these two pairs of levels couple by a J-dependent interaction, the anomalies in the effective B values shown in Fig. 4 can be explained.

As discussed in detail by Urban and Yamada (*14*) for ketene and diazomethane, the centrifugal distortion resonance between the ground state and the $v_5 = 1$ state observed for HNCS is induced by an operator

$$\hat{H}_{12}^{(5)} = -\omega_5 q_5 C_5^{ab}[J_a, J_b]_+ = -\frac{1}{2}\omega_5 q_5 C_5^{ab}[\hat{J}_+ + \hat{J}_-, \hat{J}_a]_+, \tag{4}$$

where C_5^{ab} is a dimensionless parameter,

TABLE VI—*Continued*

Transition	Freq.	Δ	Transition	Freq.	Δ	Transition	Freq.	Δ	Transition	Freq.	Δ
Prn (45, 1, 45)	99.95268	-3	Rrp (29, 1, 29)	128.85808	2	Qrp (55, 2, 54)	177.21699	-49	Pr- (19, 2, -)	169.71093	-10
Prn (44, 1, 44)	100.31084	-4	Rrp (30, 1, 30)	129.27045	2	Qrp (58, 2, 57)	177.22644	-22	Pr- (18, 2, -)	170.10128	-7
Prn (43, 1, 43)	100.66979	-2	Rrp (31, 1, 31)	129.68347	-3	Qrp (66, 2, 65)	177.25342	-46	Pr- (17, 2, -)	170.49161	-14
Prn (42, 1, 42)	101.02950	-1	Rrp (32, 1, 32)	130.09730	5	Qrp (71, 2, 70)	177.27257	-42	Pr- (16, 2, -)	170.88208	-12
Prn (41, 1, 41)	101.38999	1	Rrp (33, 1, 33)	130.51171	2	Qrp (72, 2, 71)	177.27736	35	Pr- (15, 2, -)	171.27265	-7
Prn (40, 1, 40)	101.75122	0	Rrp (34, 1, 34)	130.92685	3	Qrp (76, 2, 75)	177.29457	80	Pr- (14, 2, -)	171.66316	-15
Prn (39, 1, 39)	102.11319	-2	Rrp (35, 1, 35)	131.34266	2				Pr- (13, 2, -)	172.05395	0
Prn (38, 1, 38)	102.47597	0	Rrp (36, 1, 36)	131.75913	-2	Prp (82, 2, 80)	145.27028	-11	Pr- (12, 2, -)	172.44454	-12
Prn (37, 1, 37)	102.83951	2	Rrp (37, 1, 37)	132.17637	2	Prp (81, 2, 79)	145.65577	-9	Pr- (11, 2, -)	172.83555	12
Prn (36, 1, 36)	103.20377	0	Rrp (38, 1, 38)	132.59426	2	Prp (80, 2, 78)	146.04160	19	Pr- (10, 2, -)	173.22610	-15
Prn (35, 1, 35)	103.56881	1	Rrp (39, 1, 39)	133.01280	-1	Prp (79, 2, 77)	146.42705	0	Pr- (9, 2, -)	173.61699	-14
Prn (34, 1, 34)	103.93460	1	Rrp (41, 1, 41)	133.85202	0	Prp (78, 2, 76)	146.81288	11	Pr- (8, 2, -)	174.00795	-12
Prn (33, 1, 33)	104.30114	1	Rrp (42, 1, 42)	134.27267	1	Prp (77, 2, 75)	147.19864	7	Pr- (7, 2, -)	174.39894	-14
Prn (32, 1, 32)	104.66841	-1	Rrp (43, 1, 43)	134.69405	7	Prp (76, 2, 74)	147.58457	12	Pr- (6, 2, -)	174.78999	-14
Prn (31, 1, 31)	105.03649	2	Rrp (44, 1, 44)	135.11596	-3	Prp (75, 2, 73)	147.97032	-9	Pr- (5, 2, -)	175.18111	-14
Prn (30, 1, 30)	105.40528	2	Rrp (45, 1, 45)	135.53866	-2	Prp (74, 2, 72)	148.35646	0	Pr- (4, 2, -)	175.57231	-10
Prn (29, 1, 29)	105.77479	-1	Rrp (46, 1, 46)	135.96207	1	Prp (73, 2, 71)	148.74255	-3			
Prn (28, 1, 28)	106.14593	84	Rrp (47, 1, 47)	136.38617	4	Prp (72, 2, 70)	149.12884	5	Rr- (2, 2, -)	178.31194	-10
Prn (27, 1, 27)	106.51614	2	Rrp (48, 1, 48)	136.81088	0	Prp (71, 2, 69)	149.51506	-2	Rr- (3, 2, -)	178.70349	-12
Prn (26, 1, 26)	106.88791	2	Rrp (49, 1, 49)	137.23632	0	Prp (70, 2, 68)	149.90149	3	Rr- (4, 2, -)	179.09506	-17
Prn (25, 1, 25)	107.26023	-18	Rrp (50, 1, 50)	137.66243	-1	Prp (69, 2, 67)	150.28794	3	Rr- (5, 2, -)	179.48671	-19
Prn (24, 1, 24)	107.63370	3	Rrp (51, 1, 51)	138.08922	-3	Prp (68, 2, 66)	150.67444	-1	Rr- (6, 2, -)	179.87843	-18
Prn (23, 1, 23)	108.00767	0	Rrp (52, 1, 52)	138.51672	-2	Prp (67, 2, 65)	151.06107	0	Rr- (7, 2, -)	180.27021	-15
Prn (22, 1, 22)	108.38243	3	Rrp (53, 1, 53)	138.94494	3	Prp (66, 2, 64)	151.44774	-3	Rr- (8, 2, -)	180.66204	-11
Prn (21, 1, 21)	108.75804	17	Rrp (54, 1, 54)	139.37377	0	Prp (65, 2, 63)	151.83439	-16	Rr- (9, 2, -)	181.05385	-14
Prn (20, 1, 20)	109.13408	0	Rrp (55, 1, 55)	139.80325	-7	Prp (64, 2, 62)	152.22137	-4	Rr- (10, 2, -)	181.44568	-18
Prn (19, 1, 19)	109.51106	4	Rrp (56, 1, 56)	140.23351	-4	Prp (63, 2, 61)	152.60836	1	Rr- (11, 2, -)	181.83762	-15
Prn (18, 1, 18)	109.88873	3	Rrp (57, 1, 57)	140.66443	-3	Prp (62, 2, 60)	152.99537	-1	Rr- (12, 2, -)	182.22959	-14
Prn (17, 1, 17)	110.26713	3	Rrp (58, 1, 58)	141.09598	-8	Prp (61, 2, 59)	153.38243	-5	Rr- (13, 2, -)	182.62158	-14
Prn (16, 1, 16)	110.64627	3	Rrp (59, 1, 59)	141.52831	-3	Prp (60, 2, 58)	153.76964	-3	Rr- (14, 2, -)	183.01360	-14
Prn (15, 1, 15)	111.02613	3	Rrp (60, 1, 60)	141.96127	-4	Prp (59, 2, 57)	154.15689	-5	Rr- (15, 2, -)	183.40567	-12
Prn (14, 1, 14)	111.40676	6	Rrp (61, 1, 61)	142.39493	-3	Prp (58, 2, 56)	154.54429	0	Rr- (16, 2, -)	183.79772	-17
Prn (13, 1, 13)	111.78802	0	Rrp (62, 1, 62)	142.82926	-4	Prp (57, 2, 55)	154.93166	-6	Rr- (17, 2, -)	184.19006	5
Prn (12, 1, 12)	112.17009	3	Rrp (63, 1, 63)	143.26427	-4	Prp (56, 2, 54)	155.31914	-8	Rr- (18, 2, -)	184.58206	-11
Prn (11, 1, 11)	112.55285	2	Rrp (64, 1, 64)	143.69997	-5	Prp (55, 2, 53)	155.70676	-5	Rr- (19, 2, -)	184.97397	-38
Prn (10, 1, 10)	112.93634	2	Rrp (65, 1, 65)	144.13634	-6	Prp (54, 2, 52)	156.09445	-3	Rr- (20, 2, -)	185.36651	-5
Prn (9, 1, 9)	113.32055	1	Rrp (66, 1, 66)	144.57348	0	Prp (53, 2, 51)	156.48217	-6	Rr- (21, 2, -)	185.75875	-5
Prn (8, 1, 8)	113.70549	2	Rrp (67, 1, 67)	145.01121	-2	Prp (52, 2, 50)	156.86998	-8	Rr- (22, 2, -)	186.15104	-3
Prn (7, 1, 7)	114.09115	2	Rrp (68, 1, 68)	145.44962	-5	Prp (51, 2, 49)	157.25791	-6	Rr- (23, 2, -)	186.54335	-1
Prn (6, 1, 6)	114.47752	2	Rrp (69, 1, 69)	145.88875	-4	Prp (50, 2, 48)	157.64589	-6	Rr- (24, 2, -)	186.93568	1
Prn (5, 1, 5)	114.86459	0	Rrp (70, 1, 70)	146.32832	-28	Prp (49, 2, 47)	158.03394	-8	Rr- (25, 2, -)	187.32805	5
Prn (4, 1, 4)	115.25258	18	Rrp (71, 1, 71)	146.76900	-9	Prp (48, 2, 46)	158.42208	-8	Rr- (26, 2, -)	187.72045	9
Prn (3, 1, 3)	115.64091	-2	Rrp (72, 1, 72)	147.21021	-6	Prp (47, 2, 45)	158.81027	-12	Rr- (27, 2, -)	188.11285	12
			Rrp (73, 1, 73)	147.65211	-2	Prp (46, 2, 44)	159.19860	-9	Rr- (28, 2, -)	188.50525	12
Rrp (2, 1, 2)	117.98695	-10	Rrp (74, 1, 74)	148.09461	-7	Prp (45, 2, 43)	159.58701	-6	Rr- (29, 2, -)	188.89781	28
Rrp (3, 1, 3)	118.38058	2	Rrp (75, 1, 75)	148.53782	-9	Prp (44, 2, 42)	159.97547	-5	Rr- (30, 2, -)	189.29021	25
Rrp (4, 1, 4)	118.77477	0	Rrp (76, 1, 76)	148.98180	-2	Prp (43, 2, 41)	160.36399	-7	Rr- (31, 2, -)	189.68268	29
Rrp (5, 1, 5)	119.16971	2	Rrp (77, 1, 77)	149.42637	-5	Prp (42, 2, 40)	160.75257	-10	Rr- (32, 2, -)	190.07521	37
Rrp (6, 1, 6)	119.56531	-1	Rrp (78, 1, 78)	149.87166	-4	Prp (41, 2, 39)	161.14127	-9	Rr- (33, 2, -)	190.46773	43
Rrp (7, 1, 7)	119.96170	4	Rrp (79, 1, 79)	150.31768	1	Prp (40, 2, 38)	161.53003	-9	Rr- (34, 2, -)	190.86025	48
Rrp (8, 1, 8)	120.35863	-7	Rrp (80, 1, 80)	150.76445	12	Prp (39, 2, 37)	161.91885	-11	Rr- (35, 2, -)	191.25278	52
Rrp (9, 1, 9)	120.75649	5	Rrp (81, 1, 81)	151.21161	-6	Prp (38, 2, 36)	162.30790	3	Rr- (36, 2, -)	191.64532	58
Rrp (10, 1, 10)	121.15491	2	Rrp (82, 1, 82)	151.65973	4	Pr- (37, 2, -)	162.69717	31	Rr- (37, 2, -)	192.03772	50
Rrp (11, 1, 11)	121.55405	2	Rrp (83, 1, 83)	152.10844	3	Pr- (36, 2, -)	163.08643	50	Rr- (38, 2, -)	192.42997	25
Rrp (12, 1, 12)	121.95386	-2	Rrp (84, 1, 84)	152.55785	5	Pr- (35, 2, -)	163.47558	51	Rr- (39, 2, -)	192.82231	10
Rrp (13, 1, 13)	122.35445	1	Rrp (87, 1, 87)	153.91010	-1	Pr- (34, 2, -)	163.86495	67	Rr- (40, 2, -)	193.21516	45
Rrp (14, 1, 14)	122.75571	2				Pr- (33, 2, -)	164.25398	41	Rrr (41, 2, 39)	193.60718	-2
Rrp (15, 1, 15)	123.15765	1	Qrp (6, 2, 4)	177.13878	11	Pr- (32, 2, -)	164.64328	35	Rrr (42, 2, 40)	193.99968	-1
Rrp (16, 1, 16)	123.56031	2	Qrp (50, 2, 48)	177.19805	51	Pr- (31, 2, -)	165.03266	30	Rrr (43, 2, 41)	194.39197	-21
Rrp (17, 1, 17)	123.96366	2	Qrp (53, 2, 51)	177.20358	-74	Pr- (30, 2, -)	165.42211	25	Rrr (44, 2, 42)	194.78465	-1
Rrp (18, 1, 18)	124.36770	2	Qrp (54, 2, 52)	177.20630	-34	Pr- (29, 2, -)	165.81163	19	Rrr (45, 2, 43)	195.17713	-1
Rrp (19, 1, 19)	124.77246	3	Qrp (55, 2, 53)	177.20898	0	Pr- (28, 2, -)	166.20129	20	Rrr (46, 2, 44)	195.56956	-4
Rrp (20, 1, 20)	125.17790	3	Qrp (57, 2, 55)	177.21427	51	Pr- (27, 2, -)	166.59093	12	Rrr (47, 2, 45)	195.96202	-4
Rrp (21, 1, 21)	125.58385	-15	Qrp (65, 2, 63)	177.23351	-34	Pr- (26, 2, -)	166.98066	7	Rrr (48, 2, 46)	196.35449	-1
Rrp (22, 1, 22)	125.99086	3	Qrp (74, 2, 72)	177.25774	-19	Pr- (25, 2, -)	167.37049	4	Rrr (49, 2, 47)	196.74691	-2
Rrp (23, 1, 23)	126.39838	2	Qrp (75, 2, 73)	177.26111	44	Pr- (24, 2, -)	167.76041	3	Rrr (50, 2, 48)	197.13932	-2
Rrp (25, 1, 25)	127.21549	0	Qrp (45, 2, 44)	177.19047	-25	Pr- (23, 2, -)	168.15037	0	Rrr (51, 2, 49)	197.53172	-2
Rrp (26, 1, 26)	127.62513	4	Qrp (46, 2, 45)	177.19299	-15	Pr- (22, 2, -)	168.54042	-2	Rrr (52, 2, 50)	197.92409	-3
Rrp (27, 1, 27)	128.03541	2	Qrp (47, 2, 46)	177.19555	-6	Pr- (21, 2, -)	168.93033	-24	Rrr (53, 2, 51)	198.31646	-1
Rrp (28, 1, 28)	128.44640	2	Qrp (53, 2, 52)	177.21161	-5	Pr- (20, 2, -)	169.32066	-10	Rrr (54, 2, 52)	198.70883	2

$$C_5^{ab} = [4\pi^2 h/(\omega_5 c)]^{3/2} a_5^{ab}/(2I_aI_b), \qquad (5)$$

and ω_5 is the wavenumber of the harmonic oscillation of the ν_5 mode. The standard second order perturbation treatment of the $\hat{H}_{12}$ of Eq. (4), where the rotational and vibrational motions are separately handled, results in the quadratic centrifugal distortion term in the effective rotational Hamiltonian. However, such a separation is not adequate for the present system, because the energy separation between the interacting levels coupled by $\hat{H}_{12}$ is strongly dependent on the K_a value.

TABLE VI—*Continued*

Transition	Freq.	Δ	Transition	Freq.	Δ	Transition	Freq.	Δ	Transition	Freq.	Δ
Rrr (55, 2, 53)	199.10113	1	Prn (42, 2, 41)	160.75553	-7	Qr- (66, 3, -)	228.33640	1	Pr- (37, 3, -)	213.93517	-8
Rrr (56, 2, 54)	199.49344	3	Prn (41, 2, 40)	161.14397	-5	Qr- (65, 3, -)	228.33937	1	Pr- (36, 3, -)	214.32783	-3
Rrr (57, 2, 55)	199.88567	0	Prn (40, 2, 39)	161.53259	6	Qr- (64, 3, -)	228.34231	1	Pr- (35, 3, -)	214.72044	-3
Rrr (58, 2, 56)	200.27793	4	Prn (39, 2, 38)	161.92103	-11	Qr- (63, 3, -)	228.34523	2	Pr- (34, 3, -)	215.11300	-6
Rrr (59, 2, 57)	200.67012	3	Prn (38, 2, 37)	162.30957	-26	Qr- (62, 3, -)	228.34814	5	Pr- (33, 3, -)	215.50561	-3
Rrr (60, 2, 58)	201.06233	7				Qr- (61, 3, -)	228.35099	6	Pr- (32, 3, -)	215.89820	0
Rrr (61, 2, 59)	201.45448	9	Rrp (41, 2, 40)	193.60984	-2	Qr- (60, 3, -)	228.35383	8	Pr- (31, 3, -)	216.29072	-3
Rrr (62, 2, 60)	201.84660	11	Rrp (42, 2, 41)	194.00263	1	Qr- (59, 3, -)	228.35663	10	Pr- (30, 3, -)	216.68323	-5
Rrr (63, 2, 61)	202.23863	8	Rrp (43, 2, 42)	194.39529	-10	Qr- (58, 3, -)	228.35941	14	Pr- (29, 3, -)	217.07573	-5
Rrr (64, 2, 62)	202.63046	-11	Rrp (44, 2, 43)	194.78810	-8	Qr- (57, 3, -)	228.36213	14	Pr- (28, 3, -)	217.46822	-5
Rrr (65, 2, 63)	203.02257	2	Rrp (45, 2, 44)	195.18088	-10	Qr- (56, 3, -)	228.36484	18	Pr- (27, 3, -)	217.86068	-6
Rrr (66, 2, 64)	203.41458	10	Rrp (46, 2, 45)	195.57377	-3	Qr- (55, 3, -)	228.36753	23	Pr- (26, 3, -)	218.25315	-3
Rrr (67, 2, 65)	203.80643	6	Rrp (47, 2, 46)	195.96663	1	Qr- (54, 3, -)	228.37018	26	Pr- (25, 3, -)	218.64553	-7
Rrr (68, 2, 66)	204.19830	9	Rrp (48, 2, 47)	196.35949	3	Qr- (53, 3, -)	228.37277	29	Pr- (24, 3, -)	219.03794	-5
Rrr (69, 2, 67)	204.59006	5	Rrp (49, 2, 48)	196.75232	1	Qr- (52, 3, -)	228.37530	29	Pr- (23, 3, -)	219.43030	-5
Rrr (70, 2, 68)	204.98182	7	Rrp (50, 2, 49)	197.14522	5	Qr- (51, 3, -)	228.37781	30	Pr- (22, 3, -)	219.82261	-8
Rrr (71, 2, 69)	205.37353	9	Rrp (51, 2, 50)	197.53807	3	Qr- (50, 3, -)	228.38029	33	Pr- (21, 3, -)	220.21494	-6
Rrr (72, 2, 70)	205.76517	9	Rrp (52, 2, 51)	197.93097	5	Qr- (49, 3, -)	228.38274	36	Pr- (20, 3, -)	220.60722	-5
Rrr (73, 2, 71)	206.15670	4	Rrp (53, 2, 52)	198.32387	6	Qr- (48, 3, -)	228.38521	45	Pr- (19, 3, -)	220.99948	-3
Rrr (74, 2, 72)	206.54828	9	Rrp (54, 2, 53)	198.71677	6	Qr- (47, 3, -)	228.38757	47	Pr- (18, 3, -)	221.39167	-6
Rrr (75, 2, 73)	206.93970	5	Rrp (55, 2, 54)	199.10965	4	Qr- (46, 3, -)	228.38992	52	Pr- (17, 3, -)	221.78416	25
Rrr (76, 2, 74)	207.33114	9	Rrp (56, 2, 55)	199.50261	9	Qr- (45, 3, -)	228.39209	44	Pr- (16, 3, -)	222.17598	-6
Rrr (77, 2, 75)	207.72245	6	Rrp (57, 2, 56)	199.89554	10	Qr- (43, 3, -)	228.39676	72	Pr- (15, 3, -)	222.56812	-3
Rrr (78, 2, 76)	208.11371	4	Rrp (58, 2, 57)	200.28846	9				Pr- (14, 3, -)	222.96017	-4
Rrr (79, 2, 77)	208.50489	2	Rrp (59, 2, 58)	200.68142	12	Pr- (85, 3, -)	195.10445	1	Pr- (13, 3, -)	223.35219	-5
Rrr (80, 2, 78)	208.89607	6	Rrp (60, 2, 59)	201.07439	16	Pr- (83, 3, -)	195.88694	-44	Pr- (12, 3, -)	223.74416	-7
Rrr (81, 2, 79)	209.28703	-5	Rrp (61, 2, 60)	201.46729	12	Pr- (82, 3, -)	196.27878	-15	Pr- (11, 3, -)	224.13611	-7
Rrr (82, 2, 80)	209.67843	36	Rrp (62, 2, 61)	201.86023	12	Pr- (81, 3, -)	196.67049	-6	Pr- (10, 3, -)	224.52804	-4
Rrr (83, 2, 81)	210.06890	-9	Rrp (63, 2, 62)	202.25348	43	Pr- (80, 3, -)	197.06292	70	Pr- (9, 3, -)	224.91991	-4
Rrr (84, 2, 82)	210.45988	5	Rrp (64, 2, 63)	202.64630	30	Pr- (78, 3, -)	197.84533	-40	Pr- (8, 3, -)	225.31173	-3
			Rrp (65, 2, 64)	203.03910	15	Pr- (77, 3, -)	198.23743	-12	Pr- (7, 3, -)	225.70337	-17
Prn (82, 2, 81)	145.31139	12	Rrp (66, 2, 65)	203.43216	25	Pr- (76, 3, -)	198.62928	-16	Pr- (6, 3, -)	226.09521	-5
Prn (81, 2, 80)	145.69511	29	Rrp (67, 2, 66)	203.82498	12	Pr- (75, 3, -)	199.02120	-17	Pr- (5, 3, -)	226.48711	17
Prn (80, 2, 79)	146.07882	30	Rrp (68, 2, 67)	204.21801	20	Pr- (74, 3, -)	199.41318	-17			
Prn (79, 2, 78)	146.46246	9	Rrp (69, 2, 68)	204.61104	28	Pr- (73, 3, -)	199.80526	-11	Rr- (3, 3, -)	230.00971	-5
Prn (78, 2, 77)	146.84666	29	Rrp (70, 2, 69)	205.00391	20	Pr- (72, 3, -)	200.19728	-16	Rr- (4, 3, -)	230.40083	-8
Prn (77, 2, 76)	147.23055	4	Rrp (71, 2, 70)	205.39688	21	Pr- (71, 3, -)	200.58943	-12	Rr- (5, 3, -)	230.79196	-5
Prn (75, 2, 74)	147.99933	11	Rrp (72, 2, 71)	205.78987	25	Pr- (70, 3, -)	200.98159	-11	Rr- (6, 3, -)	231.18300	-4
Prn (74, 2, 73)	148.38394	16	Rrp (73, 2, 72)	206.18282	25	Pr- (69, 3, -)	201.37376	-12	Rr- (7, 3, -)	231.57397	-5
Prn (73, 2, 72)	148.76864	15	Rrp (74, 2, 73)	206.57581	30	Pr- (68, 3, -)	201.76601	-10	Rr- (8, 3, -)	231.96488	-5
Prn (72, 2, 71)	149.15345	12	Rrp (75, 2, 74)	206.96873	26	Pr- (67, 3, -)	202.15825	-12	Rr- (9, 3, -)	232.35574	-5
Prn (71, 2, 70)	149.53852	21	Rrp (76, 2, 75)	207.36176	36	Pr- (66, 3, -)	202.55064	-3	Rr- (10, 3, -)	232.74655	-3
Prn (70, 2, 69)	149.92357	15	Rrp (77, 2, 76)	207.75471	37	Pr- (65, 3, -)	202.94275	-25	Rr- (11, 3, -)	233.13727	-4
Prn (69, 2, 68)	150.30884	17	Rrp (78, 2, 77)	208.14761	34	Pr- (64, 3, -)	203.33524	-12	Rr- (12, 3, -)	233.52793	-5
Prn (68, 2, 67)	150.69411	7	Rrp (79, 2, 78)	208.54055	35	Pr- (63, 3, -)	203.72779	4	Rr- (13, 3, -)	233.91852	-6
Prn (67, 2, 66)	151.07961	6	Rrp (80, 2, 79)	208.93364	51	Pr- (62, 3, -)	204.12010	-6	Rr- (14, 3, -)	234.30906	-6
Prn (66, 2, 65)	151.46528	9	Rrp (81, 2, 80)	209.32642	38	Pr- (61, 3, -)	204.51248	-12	Rr- (15, 3, -)	234.69954	-5
Prn (65, 2, 64)	151.85102	7	Rrp (82, 2, 81)	209.71939	43	Pr- (60, 3, -)	204.90497	-11	Rr- (16, 3, -)	235.08997	-2
Prn (64, 2, 63)	152.23691	7	Rrp (83, 2, 82)	210.11226	39	Pr- (59, 3, -)	205.29750	-7	Rr- (17, 3, -)	235.48029	-4
Prn (63, 2, 62)	152.62270	-16	Rrp (84, 2, 83)	210.50520	43	Pr- (58, 3, -)	205.69008	0	Rr- (18, 3, -)	235.87053	-7
Prn (62, 2, 61)	153.00895	-5				Pr- (57, 3, -)	206.08256	-6	Rr- (19, 3, -)	236.26076	-3
Prn (61, 2, 60)	153.39530	4	Qr- (87, 3, -)	228.26823	0	Pr- (56, 3, -)	206.47510	-7	Rr- (20, 3, -)	236.65088	-4
Prn (60, 2, 59)	153.78170	6	Qr- (86, 3, -)	228.27168	0	Pr- (55, 3, -)	206.86766	-8	Rr- (21, 3, -)	237.04094	-4
Prn (59, 2, 58)	154.16816	2	Qr- (85, 3, -)	228.27508	-4	Pr- (54, 3, -)	207.26027	-5	Rr- (22, 3, -)	237.43094	-3
Prn (58, 2, 57)	154.55473	-3	Qr- (84, 3, -)	228.27837	-16	Pr- (53, 3, -)	207.65287	-5	Rr- (23, 3, -)	237.82086	-3
Prn (57, 2, 56)	154.94148	-1	Qr- (83, 3, -)	228.28182	-11	Pr- (52, 3, -)	208.04549	-5	Rr- (24, 3, -)	238.21072	-1
Prn (56, 2, 55)	155.32834	0	Qr- (82, 3, -)	228.28519	-12	Pr- (51, 3, -)	208.43840	24	Rr- (25, 3, -)	238.60049	-1
Prn (55, 2, 54)	155.71532	2	Qr- (79, 3, -)	228.29528	-7	Pr- (50, 3, -)	208.83073	-6	Rr- (26, 3, -)	238.99020	0
Prn (54, 2, 53)	156.10236	-2	Qr- (78, 3, -)	228.29843	-22	Pr- (49, 3, -)	209.22338	-5	Rr- (27, 3, -)	239.37981	-1
Prn (53, 2, 52)	156.48954	-3	Qr- (77, 3, -)	228.30179	-14	Pr- (48, 3, -)	209.61603	-5	Rr- (28, 3, -)	239.76935	-2
Prn (52, 2, 51)	156.87688	1	Qr- (76, 3, -)	228.30511	-8	Pr- (47, 3, -)	210.00870	-4	Rr- (29, 3, -)	240.15883	-1
Prn (51, 2, 50)	157.26423	-4	Qr- (75, 3, -)	228.30833	-9	Pr- (46, 3, -)	210.40137	-2	Rr- (30, 3, -)	240.54825	1
Prn (50, 2, 49)	157.65168	-10	Qr- (74, 3, -)	228.31156	-7	Pr- (45, 3, -)	210.79402	-3	Rr- (31, 3, -)	240.93755	-1
Prn (49, 2, 48)	158.03931	-9	Qr- (73, 3, -)	228.31474	-8	Pr- (44, 3, -)	211.18667	-4	Rr- (32, 3, -)	241.32680	0
Prn (48, 2, 47)	158.42715	2	Qr- (72, 3, -)	228.31790	-8	Pr- (43, 3, -)	211.57934	-3	Rr- (33, 3, -)	241.71601	5
Prn (47, 2, 46)	158.81493	-2	Qr- (71, 3, -)	228.32107	-5	Pr- (42, 3, -)	211.97210	7	Rr- (34, 3, -)	242.10505	0
Prn (46, 2, 45)	159.20282	-6	Qr- (70, 3, -)	228.32421	-2	Pr- (41, 3, -)	212.36465	-4	Rr- (35, 3, -)	242.49407	2
Prn (45, 2, 44)	159.59081	-10	Qr- (69, 3, -)	228.32729	-2	Pr- (40, 3, -)	212.75729	-5	Rr- (36, 3, -)	242.88302	4
Prn (44, 2, 43)	159.97890	-14	Qr- (68, 3, -)	228.33036	-1	Pr- (39, 3, -)	213.14995	-3	Rr- (37, 3, -)	243.27185	2
Prn (43, 2, 42)	160.36713	-14	Qr- (67, 3, -)	228.33344	4	Pr- (38, 3, -)	213.54257	-5	Rr- (38, 3, -)	243.66059	0

In the symmetric-top approximation, the centrifugal distortion energy, $\Delta E_{\mathrm{cd}}(J, K)$, due to the $H_{12}^{(5)}$ term in Eq. (4) for the rotational levels of the ground state is thus calculated on the basis of harmonic-oscillator-symmetric-rotor wavefunctions (*14*),

$$\Delta E_{\mathrm{cd}}(J, K) = \langle v = 0; J, K | \hat{H}_{12}^{(5)} | v = 0; J, K \rangle$$

$$= \frac{\langle v = 0; J, K | \hat{H}_{12}^{(5)} | v_5 = 1; J, K+1 \rangle \times \langle v_5 = 1; J, K+1 | \hat{H}_{12}^{(5)} | v = 0; J, K \rangle}{\langle v = 0; J, K | \hat{H}_{02} + \hat{H}_{20} | v = 0; J, K \rangle - \langle v_5 = 1; J, K+1 | \hat{H}_{02} + \hat{H}_{20} | v_5 = 1; J, K+1 \rangle}$$

TABLE VI—*Continued*

Transition	Freq.	Δ	Transition	Freq.	Δ	Transition	Freq.	Δ	Transition	Freq.	Δ
Rr- (39, 3, -)	244.04930	2	Qr- (29, 4, -)	273.75568	-17	Pr- (58, 4, -)	251.87180	-10	Rr- (20, 4, -)	281.84014	1
Rr- (40, 3, -)	244.43791	3	Qr- (30, 4, -)	273.77542	3	Pr- (57, 4, -)	252.22526	-8	Rr- (21, 4, -)	282.24581	14
Rr- (41, 3, -)	244.82643	3	Qr- (31, 4, -)	273.79557	0	Pr- (56, 4, -)	252.57901	-43	Rr- (22, 4, -)	282.65186	3
Rr- (42, 3, -)	245.21488	4	Qr- (32, 4, -)	273.81639	0	Pr- (55, 4, -)	252.93413	-6	Rr- (23, 4, -)	283.05867	5
Rr- (43, 3, -)	245.60323	4	Qr- (33, 4, -)	273.83783	-2	Pr- (54, 4, -)	253.28955	-6	Rr- (24, 4, -)	283.46603	-1
Rr- (44, 3, -)	245.99147	1	Qr- (34, 4, -)	273.85997	3	Pr- (53, 4, -)	253.64564	-4	Rr- (25, 4, -)	283.87409	2
Rr- (45, 3, -)	246.37955	-10	Qr- (35, 4, -)	273.88280	12	Pr- (52, 4, -)	254.00231	-10	Rr- (26, 4, -)	284.28279	6
Rr- (46, 3, -)	246.76778	3	Qr- (36, 4, -)	273.90605	1	Pr- (51, 4, -)	254.35977	-4	Rr- (27, 4, -)	284.69201	1
Rr- (47, 3, -)	247.15582	5	Qr- (37, 4, -)	273.93002	-2	Pr- (50, 4, -)	254.71772	-15	Rr- (28, 4, -)	285.10195	6
Rr- (48, 3, -)	247.54376	6	Qr- (38, 4, -)	273.95471	3	Pr- (49, 4, -)	255.07658	-1	Rr- (29, 4, -)	285.51247	7
Rr- (49, 3, -)	247.93147	-8	Qr- (39, 4, -)	273.98001	7	Pr- (48, 4, -)	255.43592	-5	Rr- (30, 4, -)	285.92359	7
Rr- (50, 3, -)	248.31935	4	Qr- (40, 4, -)	274.00592	8	Pr- (47, 4, -)	255.79598	-3	Rr- (31, 4, -)	286.33534	9
Rr- (51, 3, -)	248.70704	6	Qr- (41, 4, -)	274.03236	0	Pr- (46, 4, -)	256.15668	-5	Rr- (32, 4, -)	286.74764	6
Rr- (52, 3, -)	249.09462	5	Qr- (42, 4, -)	274.05938	-14	Pr- (45, 4, -)	256.51807	-3	Rr- (34, 4, -)	287.57416	9
Rr- (54, 3, -)	249.86956	8	Qr- (43, 4, -)	274.08730	0	Pr- (44, 4, -)	256.88012	-2	Rr- (35, 4, -)	287.98830	7
Rr- (55, 3, -)	250.25683	3	Qr- (44, 4, -)	274.11574	4	Pr- (43, 4, -)	257.24288	3	Rr- (36, 4, -)	288.40309	11
Rr- (56, 3, -)	250.64408	5	Qr- (45, 4, -)	274.14475	2	Pr- (42, 4, -)	257.60623	0	Rr- (37, 4, -)	288.81842	10
Rr- (57, 3, -)	251.03122	4	Qr- (46, 4, -)	274.17437	0	Pr- (41, 4, -)	257.97026	-1	Rr- (38, 4, -)	289.23435	8
Rr- (58, 3, -)	251.41830	7	Qr- (47, 4, -)	274.20465	1	Pr- (40, 4, -)	258.33496	-2	Rr- (39, 4, -)	289.65086	5
Rr- (59, 3, -)	251.80524	4	Qr- (48, 4, -)	274.23555	2	Pr- (39, 4, -)	258.70038	3	Rr- (40, 4, -)	290.06803	9
Rr- (60, 3, -)	252.19211	4	Qr- (49, 4, -)	274.26708	5	Pr- (38, 4, -)	259.06635	-5	Rr- (41, 4, -)	290.48576	10
Rr- (61, 3, -)	252.57901	15	Qr- (50, 4, -)	274.29916	1	Pr- (37, 4, -)	259.43309	-2	Rr- (42, 4, -)	290.90408	12
Rr- (62, 3, -)	252.96559	4	Qr- (51, 4, -)	274.33190	1	Pr- (36, 4, -)	259.80049	0	Rr- (43, 4, -)	291.32291	6
Rr- (63, 3, -)	253.35218	2	Qr- (52, 4, -)	274.36523	-1	Pr- (35, 4, -)	260.16853	-1	Rr- (44, 4, -)	291.74234	2
Rr- (64, 3, -)	253.73871	4	Qr- (53, 4, -)	274.39920	1	Pr- (34, 4, -)	260.53724	-2	Rr- (45, 4, -)	292.16246	9
Rr- (65, 3, -)	254.12508	-1	Qr- (54, 4, -)	274.43376	0	Pr- (33, 4, -)	260.90666	1	Rr- (46, 4, -)	292.58309	9
Rr- (66, 3, -)	254.51135	-7	Qr- (55, 4, -)	274.46892	-1	Pr- (32, 4, -)	261.27667	-4	Rr- (47, 4, -)	293.00429	9
Rr- (67, 3, -)	254.89768	3	Qr- (56, 4, -)	274.50468	-3	Pr- (31, 4, -)	261.64737	-7	Rr- (48, 4, -)	293.42607	9
Rr- (68, 3, -)	255.28383	4	Qr- (57, 4, -)	274.54103	-6	Pr- (30, 4, -)	262.01882	-2	Rr- (49, 4, -)	293.84841	9
Rr- (69, 3, -)	255.66990	6	Qr- (58, 4, -)	274.57808	0	Pr- (29, 4, -)	262.39089	-2	Rr- (50, 4, -)	294.27139	16
Rr- (70, 3, -)	256.05577	-3	Qr- (59, 4, -)	274.61568	2	Pr- (28, 4, -)	262.76363	-1	Rr- (51, 4, -)	294.69482	11
Rr- (71, 3, -)	256.44167	1	Qr- (60, 4, -)	274.65379	-6	Pr- (27, 4, -)	263.13704	-1	Rr- (52, 4, -)	295.11883	8
Rr- (72, 3, -)	256.82738	-5	Qr- (61, 4, -)	274.69270	8	Pr- (26, 4, -)	263.51112	-1	Rr- (53, 4, -)	295.54340	5
Rr- (73, 3, -)	257.21309	-1	Qr- (62, 4, -)	274.73198	-2	Pr- (25, 4, -)	263.88587	-1	Rr- (54, 4, -)	295.96863	12
Rr- (74, 3, -)	257.59878	10	Qr- (63, 4, -)	274.77197	1	Pr- (24, 4, -)	264.26129	-1	Rr- (55, 4, -)	296.39426	5
Rr- (75, 3, -)	257.98419	2	Qr- (64, 4, -)	274.81247	-5	Pr- (23, 4, -)	264.63739	1	Rr- (56, 4, -)	296.82051	5
Rr- (76, 3, -)	258.36957	1	Qr- (65, 4, -)	274.85352	-14	Pr- (22, 4, -)	265.01413	-1	Rr- (57, 4, -)	297.24738	11
Rr- (77, 3, -)	258.75489	4	Qr- (66, 4, -)	274.89532	-7	Pr- (21, 4, -)	265.39156	0	Rr- (58, 4, -)	297.67470	8
Rr- (78, 3, -)	259.14012	7	Qr- (67, 4, -)	274.93773	3	Pr- (20, 4, -)	265.76967	1	Rr- (59, 4, -)	298.10244	-8
Rr- (79, 3, -)	259.52510	-5	Qr- (68, 4, -)	274.98070	10	Pr- (19, 4, -)	266.14839	-3	Rr- (60, 4, -)	298.53101	6
Rr- (80, 3, -)	259.91020	5	Qr- (69, 4, -)	275.02388	-19	Pr- (18, 4, -)	266.52785	0	Rr- (61, 4, -)	298.96002	10
Rr- (81, 3, -)	260.29528	22	Qr- (70, 4, -)	275.06810	-3	Pr- (17, 4, -)	266.90794	-1	Rr- (62, 4, -)	299.38954	11
Rr- (82, 3, -)	260.67957	-30	Qr- (71, 4, -)	275.11269	-7	Pr- (16, 4, -)	267.28873	1	Rr- (63, 4, -)	299.81958	12
Rr- (83, 3, -)	261.06458	-1	Qr- (73, 4, -)	275.20370	-3	Pr- (15, 4, -)	267.67015	-1	Rr- (64, 4, -)	300.25006	4
Rr- (84, 3, -)	261.44916	-5	Qr- (74, 4, -)	275.25010	2	Pr- (14, 4, -)	268.05226	0	Rr- (65, 4, -)	300.68116	5
Rr- (85, 3, -)	261.83388	16	Qr- (75, 4, -)	275.29688	-10	Pr- (13, 4, -)	268.43504	1	Rr- (66, 4, -)	301.11284	12
			Qr- (76, 4, -)	275.34408	-38	Pr- (12, 4, -)	268.81852	6	Rr- (67, 4, -)	301.54489	4
Qr- (6, 4, -)	273.48510	-7	Qr- (77, 4, -)	275.39268	19	Pr- (11, 4, -)	269.20253	-3	Rr- (68, 4, -)	301.97738	-12
Qr- (7, 4, -)	273.48990	14	Qr- (78, 4, -)	275.44129	20	Pr- (10, 4, -)	269.58734	2	Rr- (69, 4, -)	302.41085	19
Qr- (8, 4, -)	273.49504	3	Qr- (79, 4, -)	275.49040	16	Pr- (9, 4, -)	269.97276	1	Rr- (71, 4, -)	303.27844	-6
Qr- (9, 4, -)	273.50091	0	Qr- (80, 4, -)	275.53984	-11	Pr- (8, 4, -)	270.35889	4	Rr- (72, 4, -)	303.71314	-4
Qr- (10, 4, -)	273.50743	-4	Qr- (81, 4, -)	275.59028	7	Pr- (7, 4, -)	270.74567	7	Rr- (73, 4, -)	304.14850	14
Qr- (11, 4, -)	273.51477	9	Qr- (83, 4, -)	275.69208	-29	Pr- (6, 4, -)	271.13257	-45	Rr- (74, 4, -)	304.58416	12
Qr- (12, 4, -)	273.52257	2							Rr- (75, 4, -)	305.02049	29
Qr- (13, 4, -)	273.53110	3	Pr- (75, 4, -)	245.96259	-44	Rr- (4, 4, -)	275.43810	2	Rr- (76, 4, -)	305.45712	25
Qr- (14, 4, -)	273.54014	-11	Pr- (74, 4, -)	246.30530	-15	Rr- (5, 4, -)	275.83338	0	Rr- (77, 4, -)	305.89409	8
Qr- (15, 4, -)	273.55004	-3	Pr- (73, 4, -)	246.64839	-12	Rr- (6, 4, -)	276.22931	-2	Rr- (78, 4, -)	306.33189	25
Qr- (16, 4, -)	273.56064	9	Pr- (72, 4, -)	246.99216	-5	Rr- (7, 4, -)	276.62592	-1			
Qr- (17, 4, -)	273.57145	-23	Pr- (71, 4, -)	247.33647	-9	Rr- (8, 4, -)	277.02315	-2	Qr- (76, 5, -)	312.81724	-71
Qr- (18, 4, -)	273.58343	-3	Pr- (70, 4, -)	247.68145	-9	Rr- (9, 4, -)	277.42109	3	Qr- (75, 5, -)	312.84718	-4
Qr- (19, 4, -)	273.59586	-4	Pr- (69, 4, -)	248.02650	-67	Rr- (10, 4, -)	277.81961	2	Qr- (74, 5, -)	312.87617	3
Qr- (20, 4, -)	273.60906	8	Pr- (67, 4, -)	248.72018	-19	Rr- (11, 4, -)	278.21863	-14	Qr- (73, 5, -)	312.90469	-2
Qr- (21, 4, -)	273.62271	0	Pr- (66, 4, -)	249.06789	-5	Rr- (12, 4, -)	278.61860	0	Qr- (72, 5, -)	312.93272	-21
Qr- (22, 4, -)	273.63693	-16	Pr- (65, 4, -)	249.41604	-11	Rr- (13, 4, -)	279.01901	-5	Qr- (71, 5, -)	312.96068	-12
Qr- (23, 4, -)	273.65210	-2	Pr- (64, 4, -)	249.76511	9	Rr- (14, 4, -)	279.42018	2	Qr- (70, 5, -)	312.98839	6
Qr- (24, 4, -)	273.66776	-4	Pr- (63, 4, -)	250.11441	-12	Rr- (15, 4, -)	279.82192	2	Qr- (69, 5, -)	313.01616	67
Qr- (25, 4, -)	273.68407	-5	Pr- (62, 4, -)	250.46452	-18	Rr- (16, 4, -)	280.22413	-15	Qr- (68, 5, -)	313.04222	-8
Qr- (26, 4, -)	273.70108	0	Pr- (61, 4, -)	250.81575	23	Rr- (17, 4, -)	280.62736	7	Qr- (67, 5, -)	313.06909	33
Qr- (27, 4, -)	273.71881	11	Pr- (60, 4, -)	251.16694	-5	Rr- (18, 4, -)	281.03094	0	Qr- (66, 5, -)	313.09482	-3
Qr- (28, 4, -)	273.73703	8	Pr- (59, 4, -)	251.51908	-4	Rr- (19, 4, -)	281.43524	2	Qr- (65, 5, -)	313.12060	1

$$+\frac{\langle v=0;J,K|\hat{H}_{12}^{(5)}|v_5=1;J,K-1\rangle \times \langle v_5=1;J,K-1|\hat{H}_{12}^{(5)}|v=0;J,K\rangle}{\langle v=0;J,K|\hat{H}_{02}+\hat{H}_{20}|v=0;J,K\rangle - \langle v_5=1;J,K-1|\hat{H}_{02}+\hat{H}_{20}|v_5=1;J,K-1\rangle}$$

$$=\frac{1}{8}(\omega_5 C_5^{ab})^2\left\{\frac{(2K+1)^2[J(J+1)-K(K+1)]}{E_0(J,K)-E_5(J,K+1)}\right.$$

TABLE VI—*Continued*

Transition	Freq.	Δ	Transition	Freq.	Δ	Transition	Freq.	Δ	Transition	Freq.	Δ
Qr- (64, 5, -)	313.14607	11	Pr- (55, 5, -)	291.84489	4	Rr- (27, 5, -)	324.78275	4	Qr- (49, 6, -)	350.88759	15
Qr- (63, 5, -)	313.17081	-17	Pr- (54, 5, -)	292.25660	-15	Rr- (28, 5, -)	325.16274	5	Qr- (50, 6, -)	350.88146	6
Qr- (62, 5, -)	313.19569	6	Pr- (53, 5, -)	292.66820	-14	Rr- (29, 5, -)	325.54227	2	Qr- (51, 6, -)	350.87522	-1
Qr- (61, 5, -)	313.21982	-9	Pr- (52, 5, -)	293.07990	30	Rr- (30, 5, -)	325.92136	-2	Qr- (52, 6, -)	350.86870	-23
Qr- (60, 5, -)	313.24393	10	Pr- (51, 5, -)	293.49043	-11	Rr- (31, 5, -)	326.30011	3	Qr- (53, 6, -)	350.86251	1
Qr- (59, 5, -)	313.26745	7	Pr- (50, 5, -)	293.90099	-15	Rr- (32, 5, -)	326.67837	0	Qr- (54, 6, -)	350.85552	-43
Qr- (58, 5, -)	313.29051	-5	Pr- (49, 5, -)	294.31125	-16	Rr- (33, 5, -)	327.05625	3	Qr- (55, 6, -)	350.84932	6
Qr- (57, 5, -)	313.31327	-11	Pr- (48, 5, -)	294.72128	-7	Rr- (34, 5, -)	327.43370	5	Qr- (56, 6, -)	350.84274	29
Qr- (56, 5, -)	313.33579	-3	Pr- (47, 5, -)	295.13079	-17	Rr- (35, 5, -)	327.81069	3	Qr- (57, 6, -)	350.83508	-43
Qr- (55, 5, -)	313.35786	-3	Pr- (45, 5, -)	295.94905	-11	Rr- (36, 5, -)	328.18730	6	Qr- (58, 6, -)	350.82838	-6
Qr- (54, 5, -)	313.37961	2	Pr- (44, 5, -)	296.35768	-7	Rr- (37, 5, -)	328.56350	11	Qr- (59, 6, -)	350.82165	42
Qr- (53, 5, -)	313.40089	-2	Pr- (43, 5, -)	296.76591	-8	Rr- (38, 5, -)	328.93914	3	Qr- (60, 6, -)	350.81403	12
Qr- (52, 5, -)	313.42180	-5	Pr- (42, 5, -)	297.17382	-7	Rr- (39, 5, -)	329.31444	3	Qr- (61, 6, -)	350.80636	-8
Qr- (51, 5, -)	313.44244	2	Pr- (41, 5, -)	297.58137	-8	Rr- (40, 5, -)	329.68932	4			
Qr- (50, 5, -)	313.46261	-1	Pr- (40, 5, -)	297.98867	1	Rr- (41, 5, -)	330.06373	0	Pr- (51, 6, -)	330.92974	23
Qr- (49, 5, -)	313.48237	-6	Pr- (39, 5, -)	298.39536	-15	Rr- (42, 5, -)	330.43782	7	Pr- (50, 6, -)	331.32567	-30
Qr- (48, 5, -)	313.50179	-7	Pr- (38, 5, -)	298.80219	17	Rr- (43, 5, -)	330.81141	7	Pr- (48, 6, -)	332.11870	6
Qr- (47, 5, -)	313.52090	-2	Pr- (37, 5, -)	299.20809	-8	Rr- (44, 5, -)	331.18461	11	Pr- (47, 6, -)	332.51463	-23
Qr- (46, 5, -)	313.53958	-1	Pr- (36, 5, -)	299.61389	-8	Rr- (45, 5, -)	331.55734	10	Pr- (46, 6, -)	332.91099	-1
Qr- (45, 5, -)	313.55787	-1	Pr- (35, 5, -)	300.01941	0	Rr- (46, 5, -)	331.92966	12	Pr- (45, 6, -)	333.30699	-6
Qr- (44, 5, -)	313.57569	-9	Pr- (34, 5, -)	300.42453	4	Rr- (47, 5, -)	332.30152	9	Pr- (44, 6, -)	333.70309	7
Qr- (43, 5, -)	313.59327	-3	Pr- (33, 5, -)	300.82921	0	Rr- (48, 5, -)	332.67277	-11	Pr- (43, 6, -)	334.09905	14
Qr- (42, 5, -)	313.61033	-11	Pr- (32, 5, -)	301.23349	-8	Rr- (49, 5, -)	333.04399	9	Pr- (42, 6, -)	334.49489	17
Qr- (41, 5, -)	313.62719	0	Pr- (31, 5, -)	301.63757	0	Rr- (50, 5, -)	333.41455	5	Pr- (40, 6, -)	335.28591	-16
Qr- (40, 5, -)	313.64349	-6	Pr- (30, 5, -)	302.04119	-1	Rr- (51, 5, -)	333.78475	7	Pr- (39, 6, -)	335.68144	-19
Qr- (39, 5, -)	313.65953	1	Pr- (29, 5, -)	302.44439	-7	Rr- (52, 5, -)	334.15445	3	Pr- (38, 6, -)	336.07698	-11
Qr- (38, 5, -)	313.67513	2	Pr- (28, 5, -)	302.84736	1	Rr- (53, 5, -)	334.52406	32	Pr- (37, 6, -)	336.47226	-21
Qr- (37, 5, -)	313.69022	-8	Pr- (27, 5, -)	303.24975	-12	Rr- (54, 5, -)	334.89263	0	Pr- (36, 6, -)	336.86782	6
Qr- (36, 5, -)	313.70534	23	Pr- (26, 5, -)	303.65197	-6	Rr- (55, 5, -)	335.26114	5	Pr- (35, 6, -)	337.26292	-4
Qr- (35, 5, -)	313.71949	-3	Pr- (25, 5, -)	304.05383	1	Rr- (56, 5, -)	335.62930	17	Pr- (34, 6, -)	337.65821	12
Qr- (34, 5, -)	313.73355	1	Pr- (24, 5, -)	304.45520	-2	Rr- (57, 5, -)	335.99700	25	Pr- (33, 6, -)	338.05314	4
Qr- (33, 5, -)	313.74723	6	Pr- (23, 5, -)	304.85621	-4	Rr- (58, 5, -)	336.36391	-1	Pr- (32, 6, -)	338.44792	-11
Qr- (32, 5, -)	313.76031	-10	Pr- (22, 5, -)	305.25691	0	Rr- (59, 5, -)	336.73076	8	Pr- (31, 6, -)	338.84290	2
Qr- (31, 5, -)	313.77312	-12	Pr- (21, 5, -)	305.65714	-4	Rr- (60, 5, -)	337.09697	-5	Pr- (30, 6, -)	339.23753	-10
Qr- (30, 5, -)	313.78568	-1	Pr- (20, 5, -)	306.05700	-8	Rr- (61, 5, -)	337.46273	-19	Pr- (29, 6, -)	339.63244	15
Qr- (29, 5, -)	313.79766	-9	Pr- (19, 5, -)	306.45646	-12	Rr- (62, 5, -)	337.82898	57	Pr- (28, 6, -)	340.02709	24
Qr- (28, 5, -)	313.80940	0	Pr- (18, 5, -)	306.85574	2	Rr- (63, 5, -)	338.19365	19	Pr- (27, 6, -)	340.42083	-49
Qr- (27, 5, -)	313.82067	1	Pr- (17, 5, -)	307.25467	20	Rr- (64, 5, -)	338.55804	-6	Pr- (26, 6, -)	340.81489	-81
Qr- (26, 5, -)	313.83151	-1	Pr- (16, 5, -)	307.65280	-3	Rr- (65, 5, -)	338.92241	10	Pr- (25, 6, -)	341.20953	-45
Qr- (25, 5, -)	313.84200	1	Pr- (15, 5, -)	308.05076	-5	Rr- (66, 5, -)	339.28637	28	Pr- (24, 6, -)	341.60341	-75
Qr- (24, 5, -)	313.85211	5	Pr- (14, 5, -)	308.44833	-6	Rr- (67, 5, -)	339.64945	-1	Pr- (23, 6, -)	341.99812	-12
Qr- (23, 5, -)	313.86178	6	Pr- (13, 5, -)	308.84537	-22	Rr- (68, 5, -)	340.01295	56	Pr- (22, 6, -)	342.39223	-1
Qr- (22, 5, -)	313.87093	-6	Pr- (12, 5, -)	309.24250	10				Pr- (21, 6, -)	342.78609	-4
Qr- (21, 5, -)	313.87980	-6	Pr- (11, 5, -)	309.63882	1	Qr- (20, 6, -)	351.00915	34	Pr- (20, 6, -)	343.17988	-5
Qr- (20, 5, -)	313.88813	-20	Pr- (10, 5, -)	310.03479	-4	Qr- (21, 6, -)	351.00673	40	Pr- (19, 6, -)	343.57360	-2
Qr- (19, 5, -)	313.89647	7	Pr- (9, 5, -)	310.43059	12	Qr- (22, 6, -)	351.00402	30	Pr- (18, 6, -)	343.96695	-25
Qr- (18, 5, -)	313.90414	7	Pr- (8, 5, -)	310.82562	-7	Qr- (23, 6, -)	351.00141	41	Pr- (17, 6, -)	344.36060	-10
Qr- (17, 5, -)	313.91140	7				Qr- (24, 6, -)	350.99855	40	Pr- (16, 6, -)	344.75397	-12
Qr- (16, 5, -)	313.91820	0	Rr- (5, 5, -)	316.31678	-6	Qr- (25, 6, -)	350.99543	24	Pr- (15, 6, -)	345.14755	18
Qr- (15, 5, -)	313.92438	-28	Rr- (6, 5, -)	316.70603	1	Qr- (26, 6, -)	350.99241	31	Pr- (13, 6, -)	345.93311	-51
Qr- (14, 5, -)	313.93073	1	Rr- (7, 5, -)	317.09481	3	Qr- (27, 6, -)	350.98938	48			
Qr- (13, 5, -)	313.93657	19	Rr- (8, 5, -)	317.48319	5	Qr- (28, 6, -)	350.98581	24	Rr- (6, 6, -)	353.77168	4
Qr- (12, 5, -)	313.94173	10	Rr- (9, 5, -)	317.87115	7	Qr- (29, 6, -)	350.98251	38	Rr- (7, 6, -)	354.16229	0
Qr- (11, 5, -)	313.94652	3	Rr- (10, 5, -)	318.25863	2	Qr- (30, 6, -)	350.97863	7	Rr- (8, 6, -)	354.55281	-1
Qr- (10, 5, -)	313.95101	8	Rr- (11, 5, -)	318.64564	-8	Qr- (31, 6, -)	350.97495	8	Rr- (9, 6, -)	354.94321	-2
Qr- (9, 5, -)	313.95467	-31	Rr- (12, 5, -)	319.03239	-3	Qr- (32, 6, -)	350.97109	3	Rr- (10, 6, -)	355.33367	17
Qr- (8, 5, -)	313.95901	39	Rr- (13, 5, -)	319.41873	2	Qr- (33, 6, -)	350.96723	10	Rr- (11, 6, -)	355.72361	-4
Qr- (7, 5, -)	313.96212	25	Rr- (14, 5, -)	319.80455	-3	Qr- (34, 6, -)	350.96321	14	Rr- (12, 6, -)	356.11364	-3
Qr- (6, 5, -)	313.96500	31	Rr- (15, 5, -)	320.19002	-1	Qr- (35, 6, -)	350.95874	-16	Rr- (13, 6, -)	356.50363	8
			Rr- (16, 5, -)	320.57506	0	Qr- (36, 6, -)	350.95417	-43	Rr- (14, 6, -)	356.89350	19
Pr- (65, 5, -)	287.70813	-33	Rr- (17, 5, -)	320.95968	0	Qr- (37, 6, -)	350.95002	-16	Rr- (15, 6, -)	357.28277	-16
Pr- (64, 5, -)	288.12325	-23	Rr- (18, 5, -)	321.34388	1	Qr- (38, 6, -)	350.94579	16	Rr- (16, 6, -)	357.67239	-3
Pr- (63, 5, -)	288.53795	-25	Rr- (19, 5, -)	321.72771	6	Qr- (39, 6, -)	350.94099	3	Rr- (17, 6, -)	358.06146	-31
Pr- (62, 5, -)	288.95266	4	Rr- (20, 5, -)	322.11094	-7	Qr- (40, 6, -)	350.93613	-4	Rr- (18, 6, -)	358.45134	35
Pr- (61, 5, -)	289.36673	0	Rr- (21, 5, -)	322.49398	3	Qr- (41, 6, -)	350.93124	-2	Rr- (19, 6, -)	358.83995	-11
Pr- (60, 5, -)	289.78029	-24	Rr- (22, 5, -)	322.87645	-1	Qr- (42, 6, -)	350.92630	8	Rr- (20, 6, -)	359.22909	8
Pr- (59, 5, -)	290.19367	-35	Rr- (23, 5, -)	323.25856	0	Qr- (43, 6, -)	350.92114	8			
Pr- (58, 5, -)	290.60706	-14	Rr- (24, 5, -)	323.64017	-6	Qr- (44, 6, -)	350.91581	4			
Pr- (57, 5, -)	291.01990	-17	Rr- (25, 5, -)	324.02147	-1	Qr- (45, 6, -)	350.91045	10			
Pr- (56, 5, -)	291.43257	-5	Rr- (26, 5, -)	324.40231	0	Qr- (48, 6, -)	350.89345	9			

$$+\frac{(2K-1)^2[J(J+1)-K(K-1)]}{E_0(J,K)-E_5(J,K-1)}\Bigg\}, \quad (6)$$

where $E_0(J,K) - E_5(J,K\pm 1)$ in the denominators are the energy differences between the interacting rovibrational levels. K again represents K_a. With the second-order perturbation expression given above, we were able to explain the observed anomalies in the effective B values; the interaction matrix elements are sufficiently small compared to the denominator in Eq. (6) and thus can be handled by the perturbation treatment. The resonance effect, as well as the avoided level-crossing effect, is interpreted by the strong K dependence of the denominators.

TABLE VII

Newly Observed Submillimeter-Wave Lines of HNCS in MHz[a]

Transition	Freq.	Δ	Transition	Freq.	Δ
Rqr (75, 0, 75)	889248.997	3	Rqr (75, 2, 74)	889624.696	-9
Rqr (76, 0, 76)	900891.679	-3	Rqr (76, 2, 75)	901273.973	11
Rqr (80, 0, 80)	947439.425	-1	Rqr (80, 2, 79)	947848.610	2
Rqr (81, 0, 81)	959070.465	2	Rqr (90, 2, 89)	1064118.466	-2
Rqr (85, 0, 85)	1005570.154	18			
Rqr (87, 0, 87)	1028804.865	-10	Rqr (75, 3, -)	889753.492	52
Rqr (88, 0, 88)	1040418.362	-6	Rqr (76, 3, -)	901404.827	39
			Rqr (80, 3, -)	947987.880	-73
Rqr (75, 1, 75)	888013.733	79	Rqr (81, 3, -)	959627.929	-126
Rqr (76, 1, 76)	899642.087	74			
Rqr (80, 1, 80)	946133.235	43	Rqr (75, 4, -)	889656.457	-1
Rqr (81, 1, 81)	957750.320	41	Rqr (76, 4, -)	901307.117	1
Rqr (85, 1, 85)	1004194.916	-28	Rqr (80, 4, -)	947887.728	1
Rqr (87, 1, 87)	1027402.623	-42	Rqr (81, 4, -)	959527.230	-1
Rqr (75, 1, 74)	890842.021	33	Prp (30, 0, 30)	944663.104	11
Rqr (76, 1, 75)	902506.288	24	Prp (25, 0, 25)	1005559.487	-6
Rqr (80, 1, 79)	949140.601	4	Prp (24, 0, 24)	1017690.465	-14
Rqr (81, 1, 80)	960793.336	-5	Prp (23, 0, 23)	1029805.234	-5
Rqr (85, 1, 84)	1007380.045	-38	Prp (22, 0, 22)	1041903.741	20
Rqr (87, 1, 86)	1030658.421	-84	Prp (21, 0, 21)	1053985.868	-6
Rqr (75, 2, 73)	889670.824	-2			
Rqr (76, 2, 74)	901321.885	3			
Rqr (80, 2, 78)	947904.165	0			
Rqr (81, 2, 79)	959544.102	-8			
Rqr (87, 2, 85)	1029334.343	12			
Rqr (90, 2, 88)	1064196.370	-6			

a) For notation see Table VI. The observed-calculated values are in the columns of Δ in kHz.

Ignoring the J dependence in the denominator of Eq. (6), which is much smaller than the K dependence, the shift in the effective B value for each K state due to the $\hat{H}_{12}$ interaction has been calculated. The denominators were evaluated from the observed K-rotational term values of the ground and the excited states given in Fig. 5. The energy of the $K_a = 7$ and 8 levels of the $v_5 = 1$ state were roughly estimated by extrapolation to be 1633 and 1984 cm^{-1}, respectively. By an iterative procedure, with the assumption that $\omega_5 = 469.2\ \text{cm}^{-1}$, the dimensionless interaction coefficient C_5^{ab} has been determined to be $5.41(5) \times 10^{-5}$, by requiring the deperturbed B values to be dependent on K, but as smooth as possible. The estimated deperturbed B values are also indicated in Fig. 4 by open circles.

VI. DISCUSSION

Figure 6 illustrates the K_a dependence of the effective B values of DNCS, where no crossing of the energy levels is expected between the ground and the lowest excited bending state in the observed range of the quantum number K_a. More rigorously, it

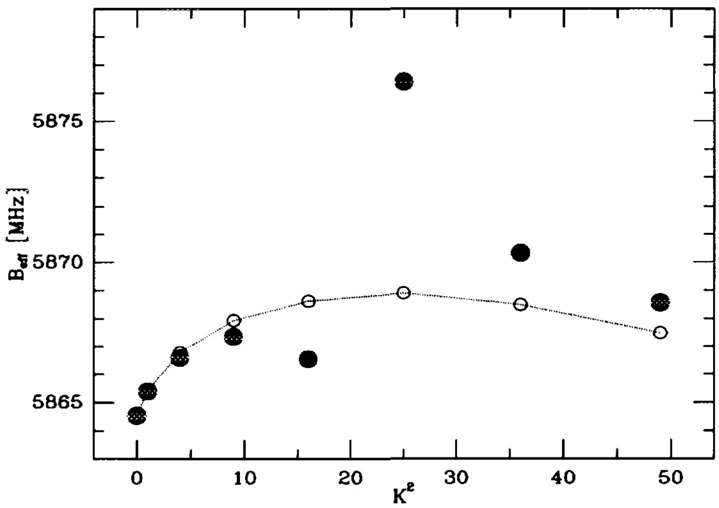

FIG. 4. The anomalous K_a dependence of the effective rotational constant B for each K_a is shown. The solid circles indicate the experimental values. For these substates, where the K doubling has been observed, the average of the two components is used for the plot. By removing the contributions from the centrifugal distortion resonance, the open circles represent the deperturbed B values.

should be mentioned that the exact locations of the rotational levels of the lowest excited state of DNCS are still unknown. However, an estimation from the vibrational energy obtained by the low-resolution infrared spectra reported by Draper and Werner (*15*) suggests that the energy separations of the interacting levels should be much larger in DNCS than in HNCS, because of the smaller rotational constant A. Thus, as expected, the effective B values of DNCS depend on K_a very smoothly, and no resonance effect can be detected. The standard theory predicts a closely linear behavior of B in dependence on K_a^2, with a slope represented by the centrifugal correction constant D_{JK}. However, the plotted B values (Fig. 6) deviate markedly from linearity. This nonlinear K_a^2 dependence is caused mainly by the quasilinearity effect, but also in part by the centrifugal distortion resonance.

A similar, but more pronounced, nonlinear K_a^2 dependence has been observed also in HNCS for the deperturbed B values, as shown in Fig. 4, where the nonlinearity is more dramatic. Since the reduced mass for the quasilinear bending vibration is much smaller in HNCS than in DNCS, one expects that the ground state level of HNCS is higher and closer to the top of the potential hump than that of DNCS, as shown in Fig. 3 of Ref. (*8*). This behavior is due to the zero-point vibrational effect. Consequently, the anomaly due to the quasilinearity is expected to be larger in HNCS.

In the rotational structure of HNCS, the combined effects of the centrifugal distortion resonance and quasilinearity find their clearest visible expression in the different degradings of the individual Q branches (see Fig. 1). Commencing with the ${}^rQ_2$ branch through ${}^rQ_6$, the direction of the degrading changes from blue to red, back to blue for ${}^rQ_4$, and again to red for ${}^rQ_5$. Finally, the ${}^rQ_6$ and presumably all higher-K_a Q branches are degraded to the red, as one normally would have expected to hold for all Q branches, in which case HNCS would be a *well behaved* close prolate rotor.

The influence of quasilinearity on the centrifugal distortion resonance can be estimated from a comparison of the magnitude of the centrifugal distortion resonance parameter C_5^{ab}. For HNCS, $C_5^{ab} = 5.41(5) \times 10^{-5}$ compares with $C_9^{ab} = 15.8 \times 10^{-5}$

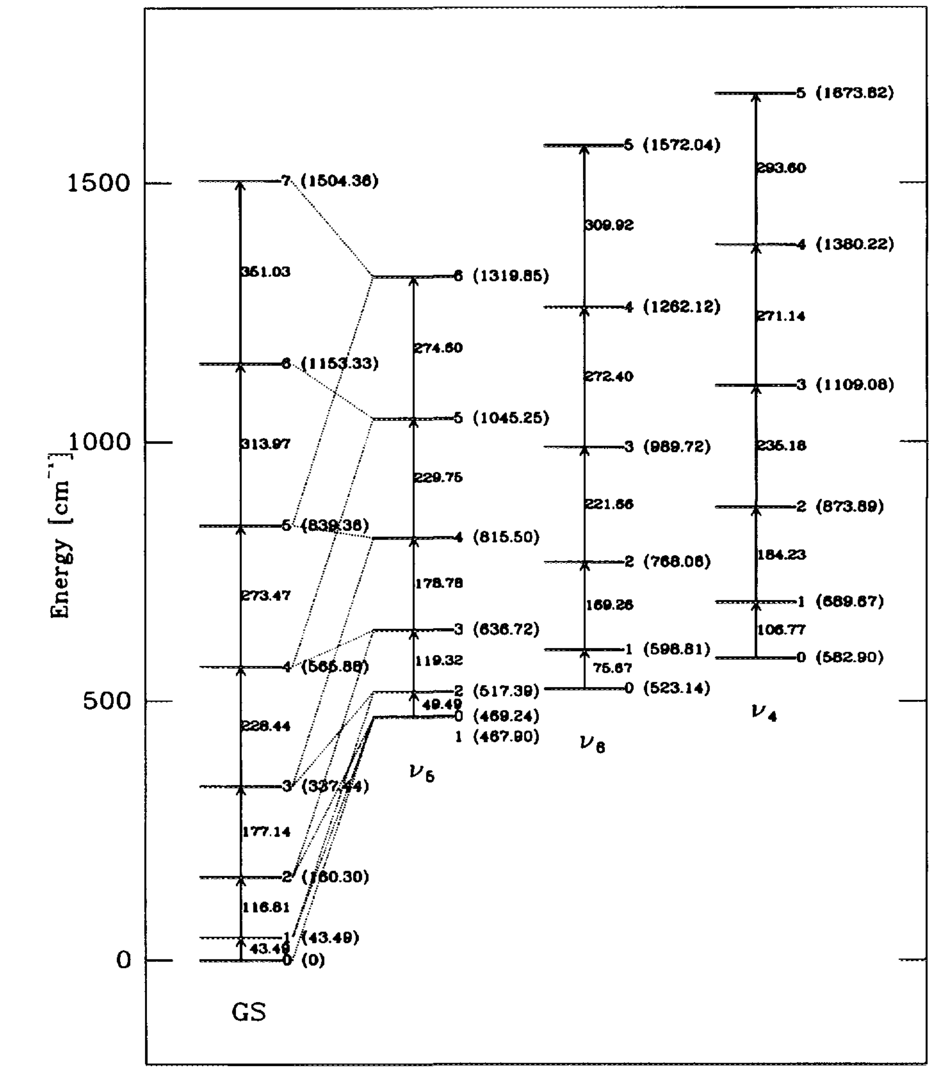

FIG. 5. The K_a rotational levels are plotted for the ground state and the three lowest bending states of HNCS. The near-resonance condition can be seen for the ground state ($K_a = 5$ level) and the $v_5 = 1$ state ($K_a = 4$ level). Details of the excited states will be presented in a forthcoming paper.

of diazomethane (*14*), $C_9^{ab} = 15.1 \times 10^{-5}$ of ketene (*14*), $C_5^{ab} = 7.9309(13) \times 10^{-5}$ of HNNN (*16*), and $C_5^{ab} = 8.09 \times 10^{-5}$ of HNCO (*17*). They are of same order of magnitude; even this parameter is smaller for HNCS or HNCO, typical quasilinear molecules, than for ketene or diazomethane. This fact indicates that the centrifugal distortion resonance is independent of the property of molecular quasilinearity. Centrifugal distortion resonance is a general interaction for a large variety of molecules, as was stated in Ref. (*7*); it becomes relevant in the ground state spectra if the rotational constant A is relatively large compared to the lowest vibrational energy. Its effect can even be observed if the energy difference between the two vibrational states coupled by this interaction is small enough.

Hegelund and Bendtsen (*16*) have analyzed the ground state rotational levels of HNNN simultaneously with the two lowest bending excited states, where they have

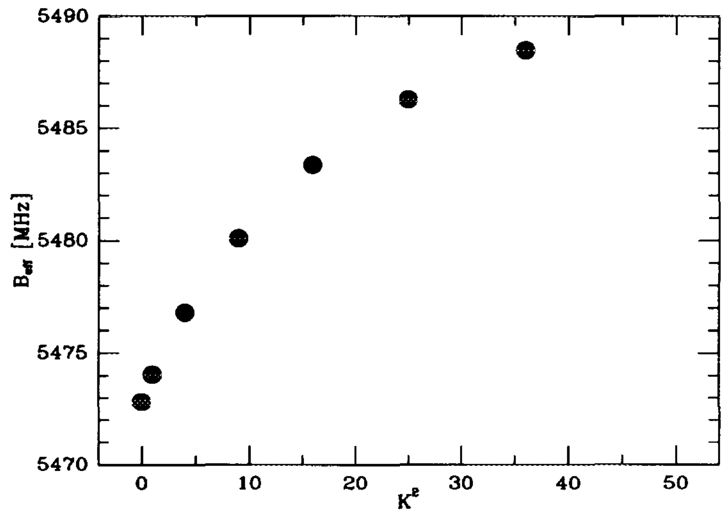

FIG. 6. The K_a dependence of the effective B values of DNCS is shown on the same scale as that used in Fig. 4. Although present in DNCS, the resonance effect is not as obvious as in HNCS. The observed K_a dependence, however, is caused by the combined effects of centrifugal distortion resonance and quasilinearity. The latter effect is more important for the observed K_a states in DNCS.

used Watson-type effective rotational Hamiltonians for each vibrational state, and have taken into account the Coriolis interactions between the two excited states and the centrifugal distortion resonance between the ground state and the lowest excited state. Such an analysis, which would be desirable for the present treatment, has not been done in this study because of the following difficulties. First, since the quasilinear effect is much larger for HNCS than for HNNN, a Watson-type effective rotational Hamiltonian for asymmetric tops is not appropriate to represent the rotational levels, even for the deperturbed ground state. Second, in HNCS there are three excited bending states (ν_4, ν_5, ν_6), instead of two, coupled together by strong Coriolis interactions (Fig. 5). One of the three states (ν_4) is the first excited state of the quasilinear bending mode, and the vibrational energy level of this state is close to the top of the potential barrier. Thus, compared to the ground state, much stronger anomalies are expected in the rotational energies of ν_4 due to the quasilinearity.

In this study, we presented the effective molecular parameters for each K_a rotational state, which can reproduce the observed line positions. In other words, for the first time, we can reproduce the observed energy levels up to $K_a = 7$ for HNCS, up to $K_a = 6$ for DNCS, and up to $K_a = 5$ for $HNC^{34}S$. Reliable rotational constants A, B, and C for these three isotopomers could be determined by applying a Watson-type Hamiltonian for the low-K_a lines, which confirm the previously reported values (5). The revision of the rotational constants in the present work does not seem to require a revision of the r_s structure (5).

ACKNOWLEDGMENTS

The authors express their thanks to the spectroscopy group of Professor Manfred Winnewisser for their support during the measurements. Especially, the assistance of Dr. S. Klee and Mr. G. Mellau during measurement is deeply appreciated. The work was supported in part by the Deutsche Forschungsgemeinschaft (DFG) through Special Grant SFB-301. The work of S.P.B. at Cologne was made possible by DFG through grants for the support of Eastern and Central European countries and the Republics of the former Soviet Union; this support is gratefully acknowledged.

RECEIVED: August 5, 1994

REFERENCES

1. K. Yamada and M. Winnewisser, *Z. Naturforsch. A* **31**, 139–144 (1976).
2. B. P. Winnewisser, *in* "Molecular Spectroscopy: Modern Research" (K. Narahari Rao, Ed.), Vol. 3, Academic Press, London, 1985.
3. L. B. Szalanski, M. C. L. Gerry, G. Winnewisser, K. Yamada, and M. Winnewisser, *Can. J. Phys.* **56**, 1297–1307 (1978).
4. K. Yamada, M. Winnewisser, G. Winnewisser, L. B. Szalanski, and M. C. L. Gerry, *J. Mol. Spectrosc.* **78**, 189–202 (1979).
5. K. Yamada, M. Winnewisser, G. Winnewisser, L. B. Szalanski, and M. C. L. Gerry, *J. Mol. Spectrosc.* **79**, 295–313 (1980).
6. B. Krakow, R. C. Lord, and G. O. Neely, *J. Mol. Spectrosc.* **27**, 148–176 (1968).
7. K. Yamada, *J. Mol. Spectrosc.* **81**, 139–151 (1980).
8. S. C. Ross, M. Niedenhoff, K. M. T. Yamada, *J. Mol. Spectrosc.* **164**, 432–444 (1994).
9. G. Guelachvili and K. Narahari Rao, "Handbook of Infrared Standards," Academic Press, Orlando, FL, 1986.
10. S. P. Belov, M. Liedtke, Th. Klaus, R. Schieder, A. H. Saleck, J. Behrend, K. M. T. Yamada, G. Winnewisser, and A. F. Krupnov, *J. Mol. Spectrosc.* **166**, 489–494 (1994).
11. G. Winnewisser and K. M. T. Yamada, *Vib. Spectrosc.* **1**, 263–272 (1991).
12. J. K. G. Watson, *in* "Vibrational Spectra and Structure" (J. R. Durig, Ed.), Vol. 6, Elsevier, Amsterdam, 1977.
13. K. M. T. Yamada and S. Klee, *J. Mol. Spectrosc.* **166**, 395–405 (1994).
14. S. Urban and K. M. T. Yamada, *J. Mol. Spectrosc.* **160**, 279–288 (1993).
15. G. R. Draper and R. L. Werner, *J. Mol. Spectrosc.* **50**, 369–402 (1974).
16. F. Hegelund and J. Bendtsen, *J. Mol. Spectrosc.* **124**, 306–316 (1987).
17. M. Niedenhoff, G. Winnewisser, and K. M. T. Yamada, to appear.